Inorg. Chem. **2008**, *47*, 4490−4505

Inorganic Chemistry
Article

Palladium(II) and Platinum(II) Organometallic Complexes with 4,7-dihydro-5-methyl-7-oxo[1,2,4]triazolo[1,5-*a*]pyrimidine. Antitumor Activity of the Platinum Compounds

José Ruiz,*,† María Dolores Villa,† Natalia Cutillas,† Gregorio López,† Concepción de Haro,† Delia Bautista,‡ Virtudes Moreno,§ and Laura Valencia||

Departamento de Química Inorgánica, Universidad de Murcia, E-30071- Murcia, Spain, S.U.I.C., Edificio S.A.C.E., Universidad de Murcia, E-30071-Murcia, Spain, Department de Química Inorgànica, Universitat de Barcelona, Martí i Franquès 1-11, E-08028 Barcelona, Spain, and Departamento de Química Inorgánica, Universidad de Santiago de Compostela, Avda. de las Ciencias s/n, E-15782 Santiago de Compostela, Spain

Received September 21, 2007

Palladium and platinum complexes with HmtpO (where HmtpO = 4,7-dihydro-5-methyl-7-oxo[1,2,4]triazolo[1,5-a]pyrimidine, an analogue of the natural ocurring nucleobase hypoxanthine) of the types [M(dmba)(PPh_3)(HmtpO)]ClO_4 [dmba = N,C-chelating 2-(dimethylaminomethyl)phenyl; M = Pd or Pt], [Pd(N−N)(C_6F_5)(HmtpO)]ClO_4 [*N*-*N* = 2,2′-bipyridine (bpy), 4,4′-dimethyl-2,2′-bipyridine (Me_2bpy), or *N*,*N*,*N*′,*N*′-tetramethylethylenediamine (tmeda)] and *cis*-[M(C_6F_5)$_2$(HmtpO)$_2$] (M = Pd or Pt) (head-to-head atropisomer in the solid state) have been obtained. Pd(II) and Pt(II) complexes with the anion of HmtpO of the types [Pd(tmeda)(C_6F_5)(mtpO)], [Pd(dmba)(μ-mtpO)]$_2$, and [NBu_4]$_2$[M(C_6F_5)$_2$(μ-mtpO)]$_2$ (M = Pd or Pt) have been prepared starting from the corresponding hydroxometal complexes. Complexes containing simultaneously both the neutral HmtpO ligand and the anionic mtpO of the type [NBu_4][M(C_6F_5)$_2$(HmtpO)(mtpO)] (M = Pd or Pt) have been also obtained. In these mtpO−HmtpO metal complexes, for the first time, prototropic exchange is observed between the two heterocyclic ligands. The crystal structures of [Pd(dmba)(PPh_3)(HmtpO)]$^+$, *cis*-[Pt(C_6F_5)$_2$(HmtpO)$_2$] · acetone, [Pd(C_6F_5)(tmeda)(mtpO)] · $2H_2O$, [Pd(dmba)(μ-mtpO)]$_2$, [NBu_4]$_2$[Pd(C_6F_5)$_2$(μ-mtpO)]$_2$ · CH_2Cl_2 · toluene, [NBu_4]$_2$[Pt(C_6F_5)$_2$(μ-mtpO)]$_2$ · 0.5(toluene), and [NBu_4][Pt(C_6F_5)$_2$(mtpO)-(HmtpO)] have been established by X-ray diffraction. Values of IC_{50} were calculated for the new platinum complexes *cis*-[Pt(C_6F_5)$_2$(HmtpO)$_2$] and [Pt(dmba)(PPh_3)(HmtpO)]ClO_4 against a panel of human tumor cell lines representative of ovarian (A2780 and A2780*cis*R), lung (NCI-H460), and breast cancers (T47D). At 48 h incubation time, both complexes were about 8-fold more active than cisplatin in T47D and show very low resistance factors against an A2780 cell line, which has acquired resistance to cisplatin. The DNA adduct formation of *cis*-[Pt(C_6F_5)$_2$(HmtpO)$_2$] and [Pt(dmba)(PPh_3)(HmtpO)]ClO_4 was followed by circular dichroism and electrophoretic mobility. Atomic force microscopy images of the modifications caused by these platinum complexes on plasmid DNA pB*R*322 were also obtained.

Introduction

Since the discovery of the antitumor activity of cisplatin in 1969, studies into platinum-nucleobase interactions have played an important role in the nucleobases as ligands.[1] There is also much interest in the study of palladium nucleobase complexes because they usually reproduce adequately the binding of the platinum complexes but with faster kinetics.[2] The HmtpO (4,7-dihydro-5-methyl-7-oxo[1,2,4]triazolo[1,5-*a*]pyrimidine) can be considered an analogue of the natural ocurring nucleobase hypoxanthine (Chart 1). The synthesis of the antitumor drug cisplatin analogue *cis*-[$PtCl_2$(HmtpO)$_2$]

* To whom correspondence should be addressed. E-mail: jruiz@um.es. Fax: +34 968 364148. Tel.: +34 968 367455.
† Departamento de Química Inorgánica, Universidad de Murcia.
‡ S.U.I.C., Edificio S.A.C.E., Universidad de Murcia.
§ Universitat de Barcelona.
|| Universidad de Santiago de Compostela.

(1) Lippert, B. *Coord. Chem. Rev.* **2000**, *200*−*202*, 487–516, and references cited therein.
(2) Barnham, K. J.; Bauer, C. J.; Djuran, M. I.; Mazid, M. A.; Rau, T.; Sadler, P. J. *Inorg. Chem.* **1995**, *34*, 2826–2832.

10.1021/ic701873b CCC: $40.75
Published on Web 04/30/2008

Chart 1

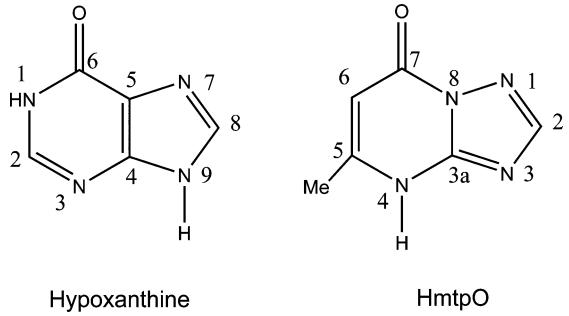

Scheme 1

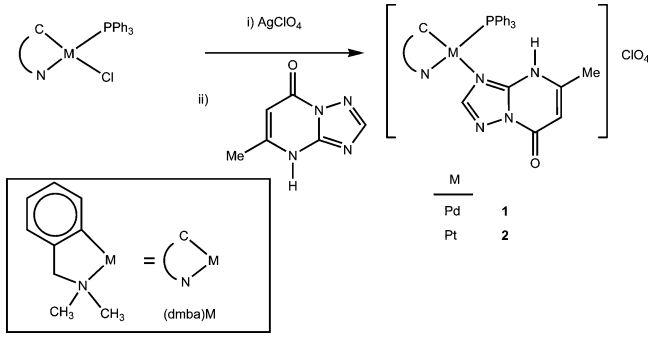

has been reported by Salas et al.,[3] and the anticancer activity of this complex has been tested against the human cancer cell lines MCF-7 breast carcinoma and A121 ovarian carcinoma. A preliminary communication on new antitumor Pt(IV) HmtpO complexes has just been reported.[4] On the other hand, because of the presence of an ionizable hydrogen at N(4), HmtpO is a well suited ligand for the study of metal−metal interactions, which give rise to homo- and heterodinuclear complexes of soft atoms such as Pt(II) and Pd(II) with metal−metal separations ranging from 2.744(2) to 3.337(1) Å.[5,6]

In the present study, our initial aim was to synthesize mononuclear and dinuclear palladium and platinum organometallic complexes derived from the N,C-chelating 2-(dimethylaminomethyl)phenyl (dmba) and pentafluorophenyl C_6F_5 groups with both the HmtpO ligand and its anion, $mtpO^-$. To the best of our knowledge,[7] the complexes herein reported represent the first examples of palladium and platinum complexes containing HmtpO and a σ-metal−carbon bond. Seven complexes have been characterized by X-ray diffraction, showing the different coordination modes of this ligand. We have also studied the interactions of some of the new platinum complexes with DNA by circular dichroism and electrophoretic mobility. Atomic force microscopy images of the modifications caused by the platinum complexes on plasmid DNA pB*R*322 were also obtained. The in vitro antiproliferative activity for the new platinum complexes *cis*-$[Pt(C_6F_5)_2(HmtpO)_2]$ and $[Pt(dmba)(PPh_3)(HmtpO)]ClO_4$ against a panel of human tumor cell lines representative of ovarian (A2780 and A2780*cis*R), lung (NCI-H460, nonsmall lung cancer cell), and breast cancers (T47D, cisplatin resistant) has been studied. At 48 h incubation time, both complexes were about 8-fold more active than cisplatin in T47D (breast cancer) and show very low resistance factors against an A2780 cell line that has acquired resistance to cisplatin.

Results and Discussion

Complexes $[M(dmba)(PPh_3)(HmtpO)]ClO_4$. The dmba complexes **1** and **2** have been prepared from the corresponding chlorometal complex $[M(dmba)(PPh_3)Cl]$ (M = Pd or Pt). After precipitation of AgCl by the addition of $AgClO_4$ in a 1:1 molar ratio in acetone, the solvent complexes $[M(dmba)(PPh_3)(Me_2CO)]ClO_4$ (M = Pd or Pt), generated in situ, react with 1 equiv of HmtpO to give the cationic complexes $[M(dmba)(PPh_3)(HmtpO)]ClO_4$ (**1**−**2**) (Scheme 1).

1 and **2** are white, air-stable solids that decompose on heating above 230 °C in a dynamic N_2 atmosphere. Their acetone solutions show conductance values corresponding to 1:1 electrolytes (Λ_M in the range 135−150 S cm^2 mol^{-1}),[8] which indicates the presence of the neutral ligand HmtpO in these complexes. An IR band is observed at ca. 1095, which is assigned to the ν_3 mode of free perchlorate (T_d symmetry). The observation of an additional band at ca. 623 cm^{-1} for the ν_4 mode confirms the presence of free perchlorate.[9] The IR spectra also show a very strong band at ca. 1715 cm^{-1} assigned to the ν(CO) of the neutral HmtpO (1680 cm^{-1} for the free ligand). The ^{1}H NMR spectra of **1** and **2** show that both the *N*-methyl and the CH_2 group of the dmba are diastereotopic, two separate signals being observed for the former and an AB quartet for the later (some broadening being observed for **1**). Therefore, there is no plane of symmetry in the palladium coordination plane. In **1** and **2**, the PPh_3-*trans*-to-NMe_2 ligand arrangement in the starting products[10,11] is preserved, after chlorine abstraction and HmtpO coordination, as can be inferred from the small, but significant, coupling constant $^4J_{P-H}$ (2.5 Hz) of one of the two CH_2N protons (resonance at δ 3.70 ppm) with the phosphorus atom[12,13] in **2**. ^{1}H NMR resonances in $CDCl_3$ of H2, H6, and CH_3 of coordinated HmtpO in **1** appear, respectively, at 0.15, 0.23, and 0.11 ppm downfield-shifted with respect to free HmtpO.

Crystal Structure of 1. The structure of **1** consists of mononuclear $[Pd(dmba)(PPh_3)(HmtpO\text{-}N^3)]^+$ cations and per-

(3) Navarro, J. A. R.; Salas, J. M.; Romero, M. A.; Vilaplana, R.; González-Vílchez, F.; Faure, R. *J. Med. Chem.* **1998**, *41*, 332–338.
(4) Lakomska, I. *J. Biol. Inorg. Chem.* **2007**, *12* (Suppl 1), S37−PO52.
(5) Navarro, J. A. R.; Romero, M. A.; Salas, J. M. *J. Chem. Soc., Dalton Trans.* **1997**, 1001–1005.
(6) Salas, J. M.; Romero, M. A.; Sánchez, M. P.; Quirós, M. *Coord. Chem. Rev.* **1999**, *195*, 1119–1142.
(7) CCDC CSD version 5.28, November 2006, update May 2007.
(8) Geary, W. J. *Coord. Chem. Rev.* **1971**, *7*, 81–122.
(9) Nakamoto, K. *Infrared and Raman Spectra of Inorganic and Coordination Compounds*, 5th ed.; Wiley-Interscience: New York, 1997; p 199.
(10) Deeming, A. J.; Rothwell, I. P.; Hursthouse, M. B.; New, L. *J. Chem. Soc., Dalton Trans.* **1978**, 1490–1496.
(11) Meijer, M. D.; Kleij, A. W.; Williams, B. S.; Ellis, D.; Lutz, M.; Spek, A. L.; van Klink, G. P. M.; van Koten, G. *Organometallics* **2002**, *21*, 264–271.
(12) Braunstein, P.; Matt, D.; Dusausoy, Y.; Fischer, J.; Mitschler, A.; Ricard, L. *J. Am. Chem. Soc.* **1981**, *103*, 5115–5125.
(13) Falvello, L. R.; Fernández, S.; Navarro, R.; Urriolabeitia, E. P. *Inorg. Chem.* **1997**, *36*, 1136–1142.

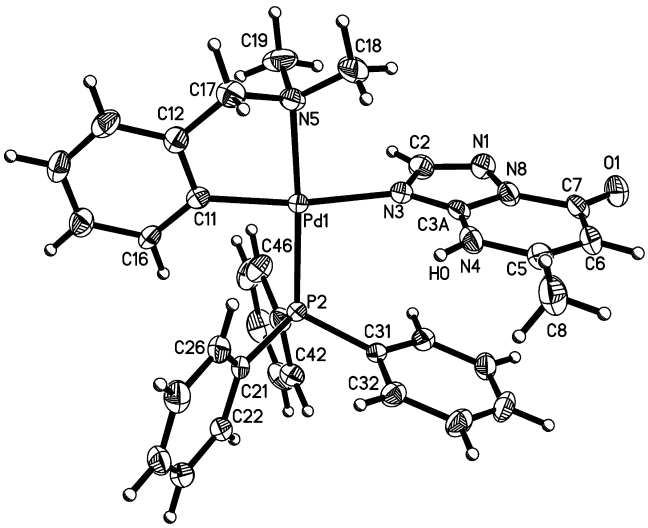

Figure 1. ORTEP representation (50% probability) of **1**. Selected bond lengths (Å) and angles (deg): Pd(1)−C(11) = 2.006(3), Pd(1)−N(5) = 2.135(3), Pd(1)−N(3) = 2.141(3), Pd(1)−P(2) = 2.2614(9), C(11)−Pd(1)−N(5) = 82.06(13), C(11)−Pd(1)−N(3) = 170.22(13), N(5)−Pd(1)−N(3) = 90.64(13), C(11)−Pd(1)−P(2) = 93.85(10), N(5)−Pd(1)−P(2) = 174.91(10), N(3)−Pd(1)−P(2) = 93.76(8).

chlorate anions. The cation of **1** is depicted in Figure 1. Coordination at palladium is approximately square planar, although the angles around palladium deviate from 90° due to the bite of the cyclometallated ligand. The C(1)−Pd−N(5) angle of 82.06(13)° is within the normal range for such complexes.[14,15] The PPh_3 ligand is trans to the nitrogen donor due to the difficulty of coordinating a phosphine trans to an aryl ligand in palladium complexes (i.e., the destabilizing effect known as transphobia).[16] The Pd−N(3) distance (2.141(3) Å) compares well with those found in the literature for palladium complexes with similar heterocyclic ligands.[17–21] The Pd−C bond length is essentially the same as that reported in [Pd(dmba)(PCy_3)(TFA)].[15] Furthermore, there is an intramolecular interaction by phenyl−HmtpO π-stacking (centroid−centroid distance, 3.611 Å).[22,23] There are also intermolecular N−H···O, C−H···N, and C−H···O bond links (distances N···4−O3, 2.830 Å; C13···N1, 3.541 Å; C17···O1, 3.317 Å; C19···O1, 3.372 Å; C19···O4, 3.344 Å; C2···O4, 3.453 Å). Intermolecular aromatic CH/π interactions[24] are found and are also responsible for the formation of extensive networks (distances H36···C13, 2.776 Å; H36···C14, 2.805 Å; H33···C14, 2.678 Å; H42···C23, 2.718 Å; and H45···C25, 2.743 Å).

Scheme 2

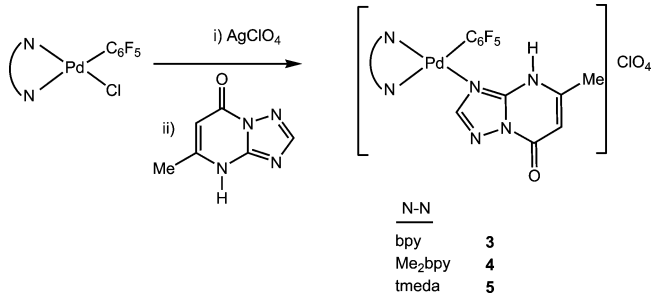

Complexes [Pd(N−N)(C_6F_5)(HmtpO)]ClO_4. In acetone, the solvent complexes [Pd(N−N)(C_6F_5)(Me_2CO)]ClO_4 [*N-N* =2,2′-bipyridine(bpy),4,4′-dimethyl-2,2′-bipyridine(Me_2bipy), or *N*,*N*,*N*′,*N*′-tetramethylethylenediamine (tmeda)] (prepared by reaction of the corresponding chloride derivatives complexes [Pd(N−N)(C_6F_5)Cl] with $AgClO_4$ in 1:1 molar ratio in acetone at room temperature) react with 1 equiv of HmtpO to yield the corresponding cationic complexes [Pd(N−N)(C_6F_5)(HmtpO)]ClO_4 (**3**−**5**) (Scheme 2) in 55−72% yields. The structures were assigned on the basis of microanalytical, IR, and ^{1}H and ^{19}F NMR data. **3**−**5** are all air-stable solids, and the thermal analysis shows that they decompose above 236 °C in a dynamic N_2 atmosphere. Their acetone solutions show conductance values corresponding to 1:1 electrolytes.[8] The IR spectra show the characteristic absorptions of the C_6F_5 group[25] at 1630, 1490, 1450, 1050, 950, and a single band at ca. 800 cm^{-1} derived from the so-called X-sensitive mode[26] in C_6F_5X (X = halogen) molecules, which is characteristic of the presence of only one C_6F_5 group in the coordination sphere of the palladium atom and behaves like a ν(M-C) band.[27] The characteristic resonances of the chelate ligands are observed in the ^{1}H NMR spectra,[27–32] and the assignments presented in the Experimental Section are based on the atom numbering given in Scheme 3. The ^{19}F NMR spectra of **3**−**5** at room temperature show hindered rotation of the C_6F_5 ring around the Pd−C

(14) Ruiz, J.; Cutillas, N.; Rodríguez, V.; Sampedro, J.; López, G.; Chaloner, P. A.; Hitchcock, P. B. *J. Chem. Soc., Dalton Trans.* **1999**, 2939–2946.
(15) Bedford, R. B.; Cazin, C. S. J.; Coles, S. J.; Gelbrich, T.; Horton, P. N.; Hursthouse, M. B.; Light, M. E. *Organometallics* **2003**, *22*, 987–999.
(16) Vicente, J.; Arcas, A.; Bautista, D.; Jones, P. G. *Organometallics* **1997**, *16*, 2127–2138.
(17) Ruiz, J.; Cutillas, N.; Vicente, C.; Villa, M. D.; López, G.; Lorenzo, J.; Avilés, F. X.; Moreno, V.; Bautista, D. *Inorg. Chem.* **2005**, *44*, 7365–7376.
(18) Lakomska, I.; Szlyk, E.; Sitkowski, J.; Kozerski, L.; Wietrzyk, J.; Pelczynska, M.; Nasulewicz, A.; Opolski, A. *J. Inorg. Biochem.* **2004**, *98*, 167–172.
(19) Szlyk, E.; Grodzicki, A.; Pazderski, L.; Wojtczak, A.; Chatlas, J.; Wrzeszcz, G.; Sitkowski, J.; Kamienski, B. *J. Chem. Soc., Dalton Trans.* **2000**, 867–872.
(20) Szlyk, E.; Lakomska, I.; Surdykowski, A.; Glowiak, T.; Pazderski, L.; Sitkowski, J.; Kozerski, L. *Inorg. Chim. Acta* **2002**, *333*, 93–99.
(21) Szlyk, E.; Pazderski, L.; Lakomska, I.; Surdykowski, A.; Glowiak, T.; Sitkowski, J.; Kozerski, L. *Polyhedron* **2002**, *21*, 343–348.
(22) Ruiz, J.; Lorenzo, J.; Sanglas, L.; Cutillas, N.; Vicente, C.; Villa, M. D.; Avilés, F. X.; López, G.; Moreno, V.; Pérez, J.; Bautista, D. *Inorg. Chem.* **2006**, *45*, 6347–6360.
(23) Janiak, C. *J. Chem. Soc., Dalton Trans.* **2000**, 3885–3896.
(24) Nishio, M. *CrystEngComm* **2004**, *6*, 130–158.
(25) Long, D. A.; Steele, D. *Spectrochim. Acta* **1963**, *19*, 1955–1961.
(26) Maslowski, E. *Vibrational Spectra of Organometallic Compounds*; Wiley: New York, 1977; 437.
(27) Ruiz, J.; Vicente, C.; Cutillas, N.; Pérez, J. *Dalton Trans.* **2005**, 1999–2006.
(28) Ruiz, J.; Martínez, M. T.; Florenciano, F.; Rodríguez, V.; López, G.; Pérez, J.; Chaloner, P. A.; Hitchcock, P. B. *Inorg. Chem.* **2003**, *42*, 3650–3661.
(29) Ruiz, J.; Martínez, M. T.; Florenciano, F.; Rodríguez, V.; López, G.; Pérez, J.; Chaloner, P. A.; Hitchcock, P. B. *Dalton Trans.* **2004**, 929–932.
(30) Ruiz, J.; Martínez, M. T.; Rodríguez, V.; López, G.; Pérez, J.; Chaloner, P. A.; Hitchcock, P. B. *Dalton Trans.* **2004**, 3521–3527.
(31) Usón, R.; Forniés, J.; Martínez, F.; Tomás, M. *J. Chem. Soc., Dalton Trans.* **1980**, 888–894.
(32) Usón, R.; Forniés, J.; Tomás, M.; Menjón, B. *Organometallics* **1985**, *4*, 1912–1914.

Scheme 3

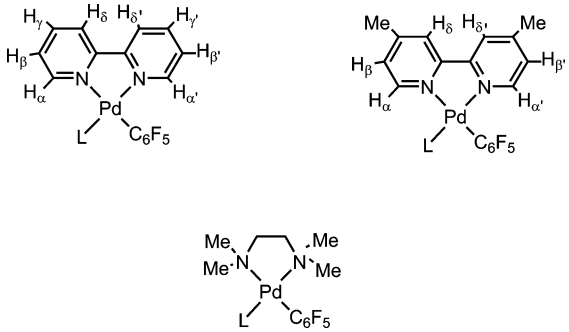

Scheme 4

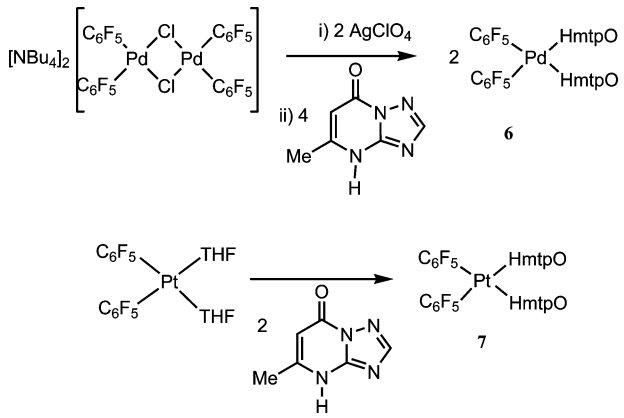

bond, and two separate signals are observed for the *o*-fluorine atoms but only one for the *p*-fluorine atom.

Complexes *cis*-[M(C_6F_5)$_2$(HmtpO)$_2$] (M = Pd or Pt). The complexes *cis*-[NBu_4]$_2$[$Pd_2(C_6F_5)_4(\mu$-Cl)$_2$][31] and *cis*-[Pt(C_6F_5)$_2$(THF)$_2$][32] are good precursors for the synthesis of **6** and **7**, respectively (Scheme 4). The reactions take place without isomerization, and the reaction products are the cis isomers. Their IR spectra show the characteristic absorptions of the C_6F_5 group (1630 m, 1490 vs, 1050 s, and 950 vs cm^{-1})[25] and a split band at ca. 800 cm^{-1} assigned to the *cis*-M(C_6F_5)$_2$ moiety.[17,26] A split band at ca. 1700 cm^{-1} is also observed for the ν(CO) of the HmtpO ligands. In any metal complex containing two equal (or similar) planar ligands occupying contiguous (cis) coordination positions, we may expect that the steric repulsion between the ligands is a minimum when the ligand planes are perpendicular to the coordination plane. If the ligands are not symmetric, there are two different situations that obey the previous condition: one of them with the analogous portion of both ligands pointing in the same direction and the other pointing to the opposite direction. These two possibilities are usually referred to as "head-head" (H−H) and "head-tail" (H−T), respectively (Figure 2). If the rotation is hindered for some reason, we can look at this situation as a special kind of isomerism, the so-called rotation isomerism or atropisomerism.[33] The H−T *cis*-[Pt(NH_3)$_2$(HmtpO-N^3)$_2$](NO_3)$_2$·2H_2O and the H−H *cis*-[$PtCl_2$(HmtpO-N^3)$_2$]·2H_2O platinum complexes have been previously reported,[4,33] which suggests that small

(33) Haj, M. A.; Quiros, M.; Salas, J. M. *J. Chem. Soc., Dalton Trans.* **2002**, 4740–4745.

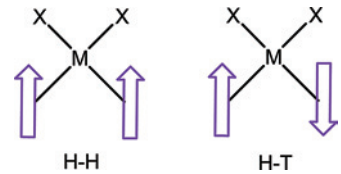

Figure 2. The two possible atropisomers in square-planar metal complexes containing two equal planar ligands occupying cis coordination positions.

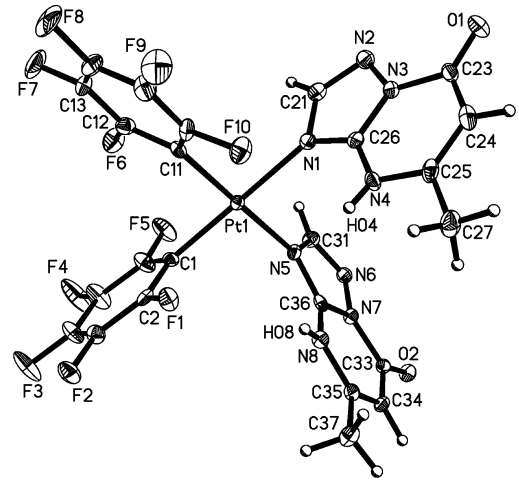

Figure 3. ORTEP representation (50% probability) of **7**·acetone. Selected bond lengths (Å) and angles (deg): Pt(1)−C(11) = 1.995(4), Pt(1)−C(1) = 1.999(4), Pt(1)−N(4) = 2.076(3), Pt(1)−N(1) = 2.089(4), C(11)−Pt(1)−C(1) = 88.79(15), C(11)−Pt(1)−N(4) = 177.80(14), C(1)−Pt(1)−N(4) = 91.41(14), C(11)−Pt(1)−N(1) = 90.94(14), C(1)−Pt(1)−N(1) = 179.44(13), N(4)−Pt(1)−N(1) = 88.84(13).

energetic contributions such as those due to hydrogen bonding or crystal packing may lead to the stabilization of different atropisomers, with the energy difference between them likewise being small.

Both the ^{1}H and ^{19}F NMR spectra of **7** in acetone-d_6 at room temperature exhibit only one set of resonances over the −60 to +60 °C range. A head−head orientation of **7** was revealed by X-ray diffraction (vide infra). On the other hand, both the ^{1}H and ^{19}F NMR spectra of **6** in acetone-d_6 at room temperature exhibit broad resonances, indicating restricted rotation about the Pd−N bonds in solution. ^{1}H and ^{19}F NMR spectra of **6** become sharp at −50 °C, rendering a unique set of resonances.

Crystal Structure of 7·acetone. Figure 3 shows the X-ray structure of **7**·acetone. Platinum is located in an almost square planar environment made up of two HmtpO ligands bonded through N3 and two ipso carbon atoms of the fluoroaryl groups. The PtN_2C_2 square has a cis configuration, which is consistent with the preparation method. The most interesting feature of this structure is the H−H orientation (Figure 4) exhibited by the HmtpO moieties (dihedral angle of 86.68°). Strong supramolecular interactions are present, and the hydrogen bond interactions N(4)−H(04)···O(2)#1 and N(8)−H(08)···O(2)#1 appear to be responsible for the H−H conformation of the molecule (N(4)···O(2)#1 contact of 2.886(5) Å; N(8)···O(2)#1 contact of 2.950(5) Å). There is also a very short intermolecular contact F1···F8 (Figure 4). In fact, the structure reported here possesses the shortest.

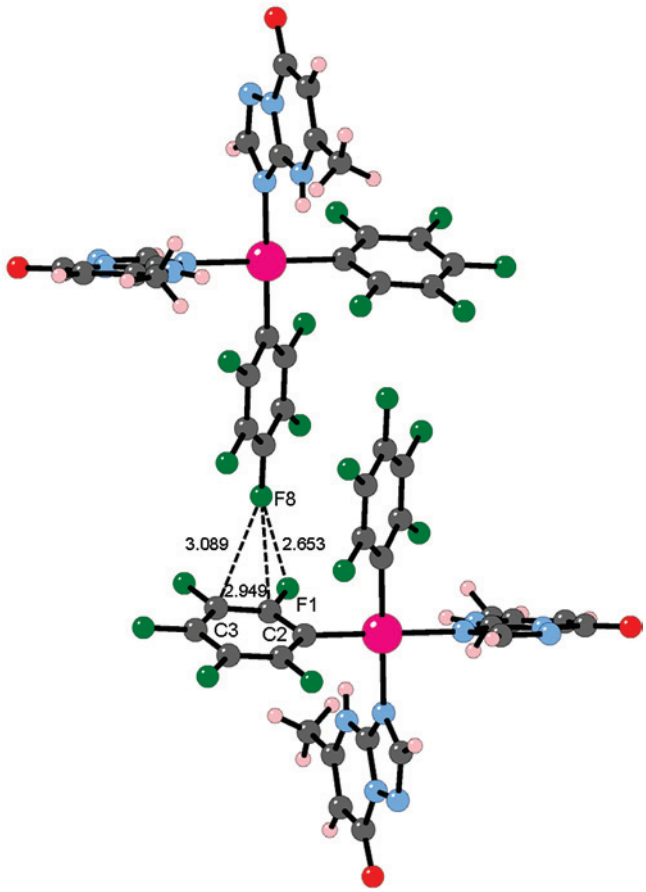

Figure 4. Intermolecular F···F and C−F···π_F interactions in **7**·acetone.

With regard to the F_{ortho}···F_{para} distance observed in fluoroaryl transition metal complexes so far (2.653 Å, Figure 4), there were no cases where F_{ortho}···F_{para} distances shorter than 2.7 Å have been previously reported.[7] The influence of these fluorine-based interactions seems to be a relevant, noncasual phenomenon to be taken into account in crystal engineering.[35,36] F8 is also involved in intermolecular C−Fπ_F interactions (F8···C2, 2.949 Å; F8···C3, 3.089 Å, Figure 4).[35,36] Other intermolecular interactions contacts observed are of the type C−H···F−C[36–40] (F4···H21, 2.341 Å; F4···H93B, 2.574 Å; F6···H31, 2.341 Å) and C−F·π_{HmtpO}[41] (F1···N6, 2.872 Å; F1···N7, 2.867 Å; F1···C33, 2.867 Å; F3···C21, 2.856 Å; F7···C35, 3.086 Å).

(34) Navarro, J. A. R.; Romero, M. A.; Salas, J. M.; Quirós, M. *Inorg. Chem.* **1997**, *36*, 3277–3283.
(35) Reichenbacher, K; Suss, H. I.; Hulliger, J. *Chem. Soc. Rev.* **2005**, *34*, 22–30.
(36) Vangala, V. R.; Nangia, A.; Lynch, V. M. *Chem. Commun.* **2002**, 1304–1305.
(37) Althoff, G.; Ruiz, J.; Rodríguez, V.; López, G.; Pérez, J.; Janiak, C. *CrystEngComm* **2006**, *8*, 662–665.
(38) Babudri, F.; Farinola, G. M.; Naso, F.; Ragni, R. *Chem. Commun.* **2007**, 1003–1022.
(39) Kasai, K.; Fujita, M. *Chem.—Eur. J.* **2007**, *13*, 3089–3105.
(40) Ruiz, J.; Villa, M. D.; Rodríguez, V.; Cutillas, N.; Vicente, C.; Lopez, G.; Bautista, D. *Inorg. Chem.* **2007**, *46*, 5448–5449.
(41) Schottel, B. L.; Chifotides, H. T.; Shatruk, M.; Chouai, A.; Perez, L. M.; Bacsa, J.; Dunbar, K. R. *J. Am. Chem. Soc.* **2006**, *128*, 5895–5912.
(42) Navarro, J. A. R.; Romero, M. A.; Salas, J. M.; Quiros, M.; Tiekink, E. R. T. *Inorg. Chem.* **1997**, *36*, 4988–4991.

Scheme 5

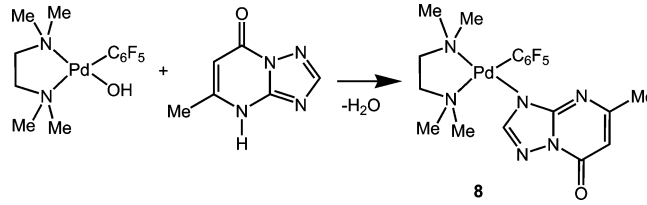

Complex [Pd(tmeda)(C_6F_5)(mtpO)]. The reaction of the hydroxopalladium complex[28] [Pd(tmeda)(C_6F_5)(OH)] in methanol with 1 equiv of HmtpO leads to the formation of [Pd(tmeda)(C_6F_5)(mtpO)] (**8**) (Scheme 5). This reaction implies proton abstraction from the HmtpO by the hydroxo complex with the concomitant release of water. The structure was assigned on the basis of microanalytical, IR, and ^{1}H and ^{19}F NMR data. **8** is an air-stable solid, and the thermal analysis shows that it decomposes above 240 °C in a dynamic N_2 atmosphere. The ^{19}F NMR spectrum of the complex at room temperature reveals the presence of a freely rotating pentafluorophenyl ring, which gives three resonances (in the ratio 2:2:1) at −121.65, −158.29, and −161.59 for the *o*-, *m*-, and *p*-fluorine atoms, respectively.

Crystal Structure of 8·2H_2O. A drawing of **8**·2H_2O is shown in Figure 5. This is the first crystal structure of a mononuclear palladium mtpO complex,[7] although some mononuclear copper mtpO complexes have been previously reported.[43,44] Coordination at palladium is approximately square planar. The mtpO ligand is approximately perpendicular to the coordination plane, with an angle between planes of 76.66°. The anionic ligand is coordinated to the palladium atom through the N(3) donor atom. The Pd−N mtpO distance [Pd(1)−N(3): 2.022(2) Å] is shorter than that observed in complex [Pd(tmeda)(C_6F_5)(1-methy)] [2.038(4) Å], suggesting a very strong interaction between the metal

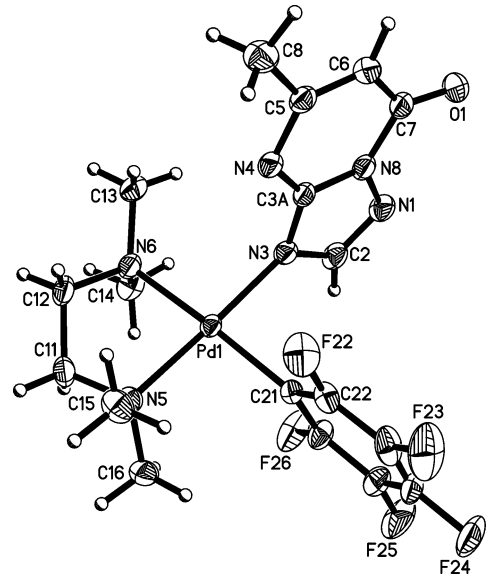

Figure 5. ORTEP representation (50% probability) of **8**·2H_2O. Selected bond lengths (Å) and angles (deg): Pd(1)−C(21) = 2.013(2), Pd(1)−N(3) = 2.022(2), Pd(1)−N(5) = 2.082(2), Pd(1)−N(6) = 2.120(2), C(21)−Pd(1)−N(3) = 86.75(9), C(21)−Pd(1)−N(5) = 94.12(9), N(3)−Pd(1)−N(5) = 176.37(8), C(21)−Pd(1)−N(6) = 173.04(9), N(3)−Pd(1)−N(6) = 94.58(9), N(5)−Pd(1)−N(6) = 84.99(9).

Scheme 6

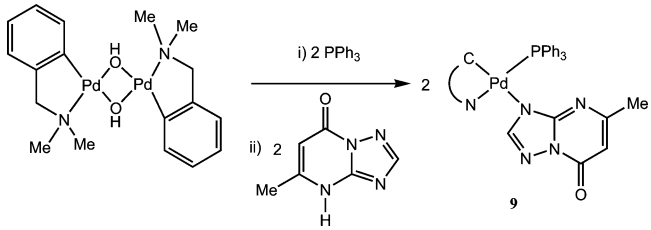

and the nitrogen.[22] The different Pd−N tmeda distances (Pd(1)−N(5): 2.082(2) Å, Pd(1)−N(6): 2.120(2) Å) are in agreement with the higher trans influence of the group C_6F_5 compared to the mtpO. The Pd−C_6F_5 bond length (2.013(2) Å) is in the range found in the literature for pentafluorophenyl−palladium complexes.[22,27] The chelate angle N(5)−Pd(1)−N(6) is 84.99(8). Intermolecular interactions contacts C−H···F−C[35–40] (F26···H16C = 2.452 Å; F26···H10 = 2.545 Å; F22···H8C = 2.599 Å; F22···H6 = 2.599 Å; F25···H2 = 2.548 Å), C−H···O−C (H13B···O1 = 2.429 Å), C−O···H−O (O1···O2 = 2.788 Å), and H−O···H−O (O2···O3 = 2.770 Å; O3···O3 = 2.740 Å) are observed.

Complex [Pd(dmba)(PPh$_3$)(mtpO)]. The reaction in dichloromethane at room temperature of the hydroxopalladium complex [Pd(dmba)(μ-OH)]$_2$[14] with PPh$_3$ and HmtpO in the molar ratio 1:2:2 leads to the formation of the mononuclear palladium complex [Pd(dmba)(PPh$_3$)(mtpO)] (**8**) (Scheme 6).

8 is a white, air-stable solid that decomposes on heating above 246 °C in a dynamic N_2 atmosphere. The structure was assigned on the basis of microanalytical, IR, and ^{1}H and ^{31}P NMR data. The ν(CO) band of the IR spectrum of **8** is observed at 1660 cm^{-1}, which is a significant difference when comparing with the values (over 1700 cm^{-1}) observed for **1**−**7**, containing the neutral HmtpO ligand. The ^{1}H NMR spectrum is temperature dependent, showing at 0 °C an AB quartet at δ 4.1 ppm for the CH_2N protons of the dmba, which indicates that these are diastereotopic (broadening being observed at room temperature, as it happens also in **1**). Therefore, there is no plane of symmetry in the palladium coordination plane.[17]

Dimeric Palladium Complexes [Pd(dmba)(μ-mtpO)]$_2$. The reaction of the hydroxopalladium complex[14] [Pd(dmba)(μ-OH)]$_2$ in dichloromethane with HmtpO (in a 1:2 ratio) leads to the formation of N(3),N(4)-bridged mtpO dipalladium complexes of the type [Pd(dmba)(μ-mtpO)]$_2$ (**10a** and **10b**) (Scheme 7). This reaction implies proton abstraction from the HmtpO ligand by the hydroxopalladium complex with the concomitant release of water. On protonation of the hydroxo complex, it is likely that an intermediate aqua complex is formed.[45]

Because both $C_6H_4CH_2NMe_2$ (dmba) and the mtpO anion are unsymmetrical, there are five possible linkage isomers for the dimeric complexes, two of them with H−H (parts d and e of Scheme 8) and the other three with H−T arrangements (parts a, b, and c of Scheme 8) of the bridging mtpO anionic ligands. Accordingly, with the ^{1}H NMR spectrum in $CDCl_3$ at room temperature, two linkage isomers (**10a** and **10b**) are present in a ratio 1:0.4. The ^{1}H NMR spectrum is not temperature dependent in the −50 to +60 °C range. The H−H isomer **10a** was isolated pure by crystallization in CH_2Cl_2/toluene/hexane of the mixture, whereas the H−L isomer **10b** was isolated pure by washing the mixture with ethanol.

Scheme 7

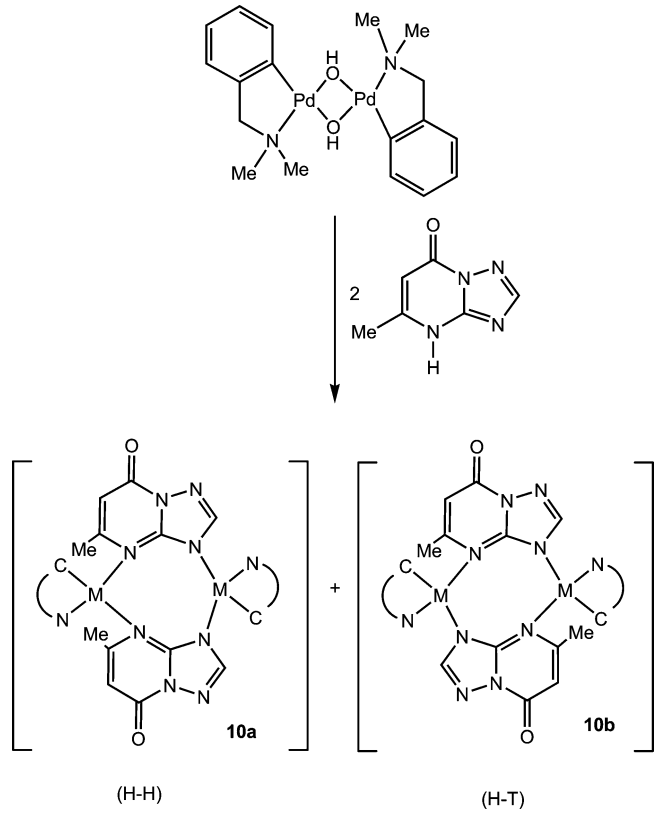

Scheme 8

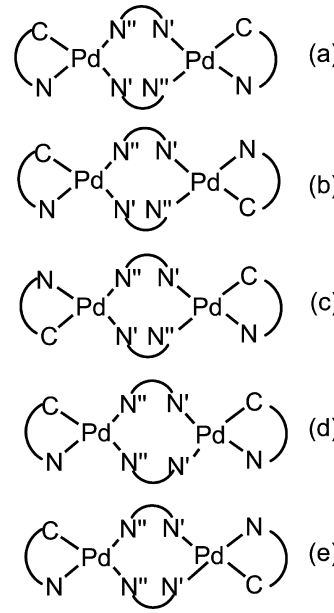

(43) Dirks, E. J.; Haasnoot, J. G.; Kinneging, A. J.; Reedijk, J *Inorg. Chem.* **1987**, *26*, 1902–1906.
(44) Navarro, J. A. R.; Romero, M. A.; Salas, J. M.; Molina, J.; Tiekink, E. R. T. *Inorg. Chim. Acta* **1998**, *274*, 53–63.
(45) Ruiz, J.; Florenciano, F.; Vicente, C.; de Arellano, M. C. R.; López, G. *Inorg. Chem. Commun.* **2000**, *3*, 73–75.

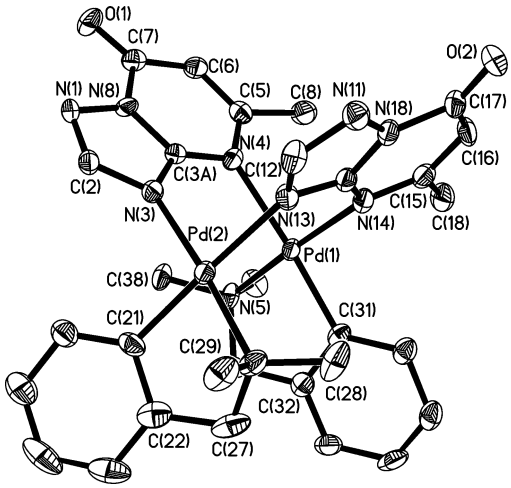

Figure 6. ORTEP representation (50% probability) of **10a**. Selected bond lengths (Å) and angles (deg): Pd(1)−C(31) = 1.989(4), Pd(1)−N(14) = 2.077(4), Pd(1)−N(5) = 2.091(4), Pd(1)−N(4) = 2.175(3), Pd(1)−Pd(2) = 3.0885(5), Pd(2)−C(21) = 1.996(4), Pd(2)−N(3) = 2.043(3), Pd(2)−N(6) = 2.080(4), Pd(2)−N(13) = 2.143(4), C(31)−Pd(1)−N(14) = 95.42(16), C(31)−Pd(1)−N(5) = 82.17(16), N(14)−Pd(1)−N(5) = 175.11(14), C(31)−Pd(1)−N(4) = 175.90(16), N(14)−Pd(1)−N(4) = 88.68(14), N(5)−Pd(1)−N(4)=93.76(14),C(21)−Pd(2)−N(3)=94.57(17),C(21)−Pd(2)−N(6) = 82.13(17), N(3)−Pd(2)−N(6) = 175.52(14), C(21)−Pd(2)−N(13) = 176.75(17), N(3)−Pd(2)−N(13) = 88.33(14), N(6)−Pd(2)−N(13) = 94.89(15).

It is well-known that the ligand dmba exerts very different trans influences through its carbon and nitrogen atoms.[46] On the other hand, Quirós et al. have recently reported[33] the synthesis of the related complex $[Pd_2(\mu\text{-tpO})_2(bpm)_2](H_5O_2)(ClO_4)_3\cdot 3H_2O$(HtpO=4,7-dihydro-7-oxo[1,2,4]triazolo-[1,5-*a*]pyrimidine; bpm = bispyrimidine), where the H−H and H−T isomers coexist even in the solid state.

The characteristic resonances of dmba were observed.[47] The ^{1}H−^{1}H COSY and HSQC-DEPT spectra enabled us to propose ^{1}H assignments for **10a** and **10b**.

Crystal Structure of 10a. In the dinuclear molecule (Figure 6), two mtpO moieties bridge the two palladium centers with an anti structure, giving rise to a Pd···Pd separation of 3.0885(5) Å, which is 0.3 Å shorter than the van der Waals radii sum. This value is in the same range as the distances found for other similar doubly bridged d^8 metal complexes[14,22,34,48] where weak attractive metal−metal interactions are present.[49,50] An H−H arrangement of the bridging mtpO anionic ligands is observed, as found previously in the heterodinuclear complex $[(NH_3)_2Pt(\mu\text{-mtpO})_2\text{-}Pd(bipy)]^{2+}$.[34] Coordination at palladium is approximately square planar with the two coordination planes inclined at 30.89° to each other giving a basket-shaped 8-membered ring. The cyclometallated rings are puckered with the nitrogen atom significantly out of the plane defined by the palladium and carbon atoms, a feature which is quite commonly observed in cyclometallated dmba complexes. The two distances Pd−N triazolo are quite different (2.043 and 2.143 Å) due to the different trans influence of the ancillary ligands (carbon and nitrogen donors). There are also C−H···N and C−H···O bond links (distances H2···N11, 2.601 Å; H18C···O1, 2.564 Å; H12···O2, 2.397 Å; H27A···O2, 2.561 Å). Other intermolecular interaction contacts observed are of the type C−H···π_{HmtpO}[24,37] (H24···N8, 2.517 Å; H14···C7, 2.740 Å; H14···N8, 2.744 Å; H38C···C7, 2.688 Å; H29A···C16, 2.757 Å).

Scheme 9

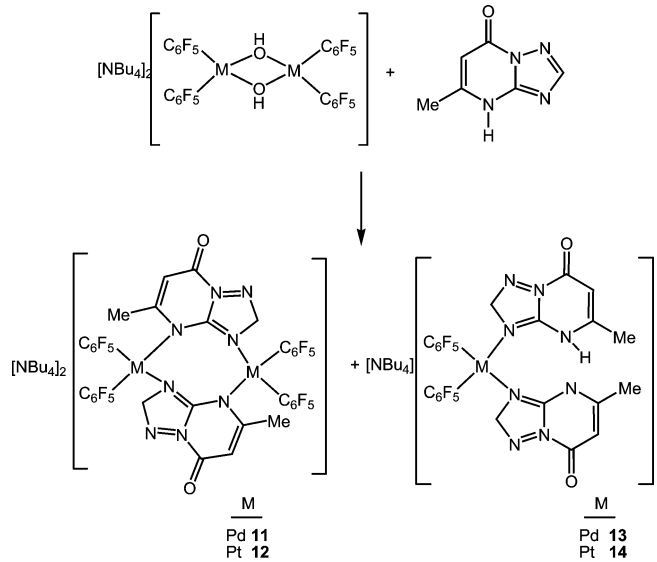

Dinuclear and Mononuclear Metal Complexes $[NBu_4]_2[M(C_6F_5)_2(\mu\text{-mtpO})]_2$ and $[NBu_4][M(C_6F_5)_2(mtpO)(HmtpO)]$ (M = Pd or Pt). The di-μ-hydroxo palladium and platinum complexes[51,52] $[NBu_4]_2[M(C_6F_5)_2(\mu\text{-OH})]_2$ react with HmtpO (in a 1:2 ratio) in acetone at room temperature for 24 h to yield a mixture containing the corresponding N(3),N(4)-bridged mtpO dinuclear complex $[NBu_4]_2[M(C_6F_5)_2(\mu\text{-mtpO})]_2$ (**11** or **12**) and the mononuclear complex $[NBu_4][M(C_6F_5)_2(mtpO)(HmtpO)]$ (**13** or **14**) (Scheme 9) in a molar ratio of approximately 1:0.4, together with starting material. When the reaction of $[NBu_4]_2[M(C_6F_5)_2(\mu\text{-OH})]_2$ (M = Pd or Pt) with HmtpO was done in a 1:4 ratio, again a mixture of the new dinuclear and mononuclear metal complexes was obtained (molar ratio of approximately 1:0.7). The platinum complexes **12** and **14** were separated mechanically after crystallization from dichloromethane/toluene/hexane. In the case of palladium, only crystals of **11** could be obtained.

11 and **12** show no indication of dynamic behavior at room temperature in the ^{1}H NMR spectrum, a unique resonance pattern for the H(2), H(6), and Me protons for the mtpO ligands

(46) Deeming, A. J.; Meah, M. N.; Bates, P. A.; Hursthouse, M. B. *J. Chem. Soc., Dalton Trans.* **1988**, 2193–2199.
(47) Ruiz, J.; Rodríguez, V.; Cutillas, N.; Pardo, M.; Pérez, J.; López, G.; Chaloner, P.; Hitchcock, P. B. *Organometallics* **2001**, *20*, 1973–1982.
(48) Krumm, M.; Mutikainen, I.; Lippert, B. *Inorg. Chem.* **1991**, *30*, 884–890.
(49) Novoa, J. J.; Aullón, G.; Alemany, P.; Alvarez, S. *J. Am. Chem. Soc.* **1995**, *117*, 7169–7171.
(50) Aullón, G.; Alemany, P.; Alvarez, S. *Inorg. Chem.* **1996**, *35*, 5061–5067.
(51) López, G.; Ruiz, J.; García, G.; Vicente, C.; Casabó, J.; Molins, E.; Miravitlles, C. *Inorg. Chem.* **1991**, *30*, 2605–2610.
(52) López, G.; Ruiz, J.; García, G.; Vicente, C.; Martí, J. M.; Hermoso, J. A.; Vegas, A.; Martínez-Ripoll, M. *J. Chem. Soc., Dalton Trans.* **1992**, 53–58.
(53) López, G.; Ruiz, J.; Vicente, C.; Martí, J. M.; García, G.; Chaloner, P. A.; Hitchcock, P. B.; Harrison, R. M. *Organometallics* **1992**, *11*, 4090–4096.

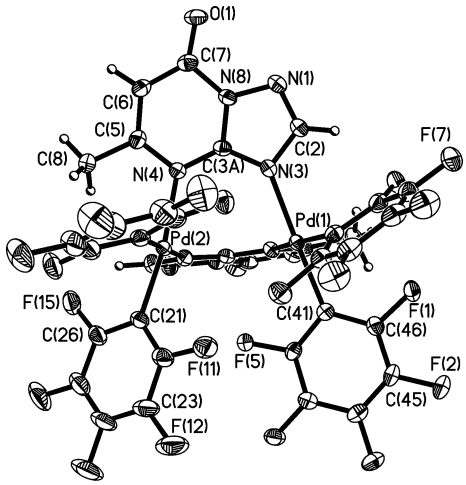

Figure 7. ORTEP representation (50% probability) of **11**·CH_2Cl_2·toluene. Selected bond lengths (Å) and angles (deg): Pd(1)−C(51) = 2.009(3), Pd(1)−C(41) = 2.012(3), Pd(1)−N(3) = 2.123(3), Pd(1)−N(14) = 2.136(3), Pd(2)−C(31) = 2.012(3), Pd(2)−C(21) = 2.014(3), Pd(2)−N(4) = 2.117(3), Pd(2)−N(13) = 2.120(3), C(51)−Pd(1)−C(41) = 86.02(13), C(51)−Pd(1)−N(3) = 91.51(11), C(41)−Pd(1)−N(3) = 177.48(11), C(51)−Pd(1)−N(14) = 170.80(12), C(41)−Pd(1)−N(14) = 91.58(11), N(3)−Pd(1)−N(14) = 90.78(10), C(31)−Pd(2)−C(21) = 86.58(14), C(31)−Pd(2)−N(4) = 90.91(12), C(21)−Pd(2)−N(4) = 171.84(12), C(31)−Pd(2)−N(13) = 178.77(13), C(21)−Pd(2)−N(13) = 93.11(12), N(4)−Pd(2)−N(13) = 89.24(11).

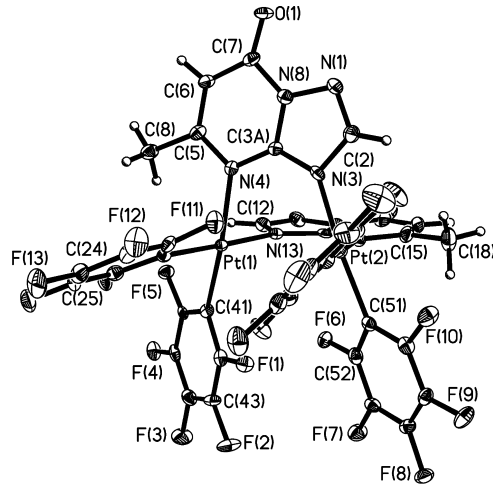

Figure 8. ORTEP representation (50% probability) of **12**·0.5(toluene). Selected bond lengths (Å) and angles (deg): Pt(1)−C(21) = 2.006(5), Pt(1)−C(41) = 2.007(5), Pt(1)−N(13) = 2.094(4), Pt(1)−N(4) = 2.122(4), Pt(2)−C(51) = 2.008(5), Pt(2)−C(31) = 2.010(5), Pt(2)−N(3) = 2.100(4), Pt(2)−N(14) = 2.105(4), C(21)−Pt(1)−C(41) = 90.5(2), C(21)−Pt(1)−N(13) = 177.92(17), C(41)−Pt(1)−N(13) = 89.57(17), C(21)−Pt(1)−N(4) = 92.64(17), C(1)−Pt(1)−N(4) = 169.95(17), N(13)−Pt(1)−N(4) = 86.99(15), C(51)−Pt(2)−C(31) = 89.57(19), C(51)−Pt(2)−N(3) = 174.81(17), C(31)−Pt(2)−N(3) = 92.74(18), C(51)−Pt(2)−N(14) = 91.29(17), C(31)−Pt(2)−N(14) = 175.18(18), N(3)−Pt(2)−N(14) = 86.02(16).

being observed, which suggests an H−T arrangement of the bridging mtpO anionic ligands. The ^{19}F NMR spectra of both complexes reveal the presence of two different types of C_6F_5 groups resonances due to the asymmetric nature of mtpO. As expected, the *ortho*-F signals of complex 12 are flanked by the satellite due to coupling to ^{195}Pt.

13 and **14** contain simultaneously both the neutral HmtpO and the anionic mtpO ligands, and they are formulated as $[NBu_4][Pt(C_6F_5)_2(mtpO)(HmtpO)]$. However, the ^{1}H NMR spectrum in $CDCl_3$ over the −60 to +25 °C range of temperature of both complexes suggests that both heterocyclic ligands are equivalent because only one set of proton resonances for them is observed. The same conclusion is inferred from the ^{19}F NMR spectra of **13** and **14**, only one resonance being observed for the *para*-F of the two pentafluorophenyl rings. This is the first time that prototropic exchange is observed between the two heterocyclic ligands for mtpO−HmtpO complexes, although exchange between the two pyrazolyl rings of azole−azolate metal complexes has been previously reported.[53]

Crystal Structures of 11·CH_2Cl_2·toluene and 12·0.5(toluene). The structure of **11**·CH_2Cl_2·toluene and **12**·0.5(toluene) are dinuclear (Figures 7 and 8), with the two mtpO ligands arranged in a H−T orientation bridging the two metal centers. The metal···metal separation in these complexes is very long (3.560 and 3.465 Å, for **11**·CH_2Cl_2·toluene and **12**·0.5(toluene), respectively) compared to that observed in **10a** (3.0885 Å) and $[Pd_2(\mu\text{-mtpO})_2(bipy)_2][NO_3]\cdot 5H_2O$ [3.034(1) Å].[5] The coordination planes of the two metal atoms in **11**·CH_2Cl_2·toluene and **12**·0.5(toluene) form a dihedral angle of 50.72 and 46.48°, respectively. The metal−N distances are in good agreement with the values found in **10a** and in other dinuclear metal mtpO complexes.[5,34] C−HO and C−HF intermolecular interactions are present in both complexes (Tables 1 and 2).

Table 1. Hydrogen Bonds for **11**·CH_2Cl_2·Toluene (Angstroms and Degrees)[a]

D−H···A	d(D−H)	d(H···A)	d(D···A)	<(DHA)
C(65)−H(65A)···O(2)	0.99	2.34	3.243(4)	150.8
C(81)−H(81A)···O(1)	0.99	2.48	3.383(4)	151.5
C(93)−H(93A)···O(1)	0.99	2.37	3.276(5)	151.5
C(85)−H(85B)···F(2)#1	0.99	2.35	3.317(4)	164.5
C(93)−H(93B)···O(1)#2	0.99	2.36	3.351(5)	174.5
C(73)−H(73A)···F(12)#3	0.99	2.45	3.442(4)	175.6
C(65)−H(65B)···O(2)#4	0.99	2.51	3.485(5)	166.7

[a] Symmetry transformations used to generate equivalent atoms: #1 $-x+1, -y+2, -z+1$; #2 $-x+1, -y+2, -z$; #3 $x+1, y, z$; #4 $-x+1, -y+1, -z+1$.

Table 2. Hydrogen Bonds for **12**·0.5(Toluene) (Angstroms and Degrees)[a]

D−H···A	d(D−H)	d(H···A)	d(D···A)	<(DHA)
C(89)−H(89B)···O(1)	0.99	2.54	3.436(7)	150.5
C(81)−H(81A)···O(1)	0.99	2.45	3.390(6)	157.7
C(81)−H(81B)···O(1)#1	0.99	2.27	3.211(6)	157.6
C(85)−H(85A)···F(18)#2	0.99	2.40	3.348(6)	160.5
C(91)−H(91A)···F(16)#3	0.99	2.55	3.504(7)	162.0
C(66)−H(66B)···F(2)#4	0.99	2.41	3.374(6)	163.2
C(65)−H(65A)···O(2)#5	0.99	2.14	3.075(6)	156.5

[a] Symmetry transformations used to generate equivalent atoms: #1 $-x+2, -y+1, -z+1$; #2 $x, y, z-1$; #3 $-x+1, -y+1, -z+1$; #4 $x+1/2, -y+3/2, z-1/2$; #5 $x+1/2, -y+3/2, z+1/2$.

In **11**·CH_2Cl_2·toluene also, intermolecular contacts F3−F8 (2.925 Å) are observed giving a centrosymmetric dimer-of-dimers arrangement (Figure 9), whereas intermolecular contacts F5−F9 (2.853 Å) in **12**·0.5(toluene) lead to 1D chains (Figure 10).

Crystal Structure of 14. The structure of the anion of **14** is shown in Figure 11. This complex is formulated as $[NBu_4][Pt(C_6F_5)_2(mtpO)(HmtpO)]$. The coordination at platinum is square-planar with interbond angles that deviate little from 90°. Two different distances Pt−N are observed

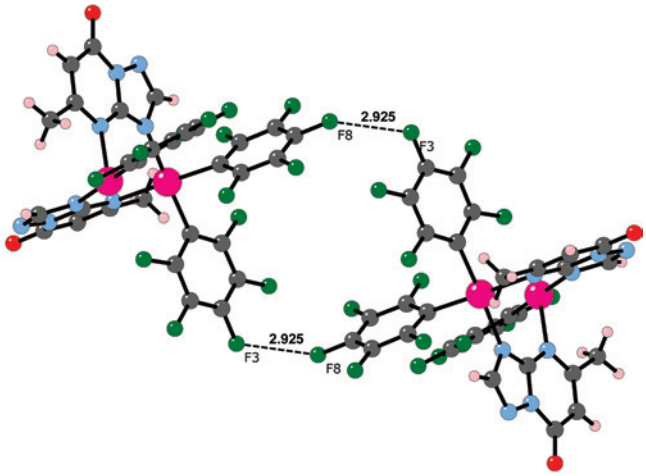

Figure 9. Centrosymmetric dimer-of-dimers arrangement of **11**·CH_2Cl_2·toluene.

[(Pt(1)−N(1) = 2.072(4) Å, Pt(1)−N(11) = 2.096(4) Å]. The dihedral angle between the heterocyclic planar ligands is 84.31°.

There are intermolecular $\pi-\pi$ interactions between mtpO ligands, so molecules of complex **14** are stacked to give centrosymmetric pairs, as shown in Figure 12. The centroid−centroid distance is 3.507 Å for the best overlapped rings, which is at the low end of the range defined for this type of interaction (3.4−3.8 Å).[23] The interplanar distance is 3.313 Å. It is a slipped packing with a deviation of the center−center line of the perpendicular of the plane of 20°.

Intermolecular interactions contacts C−H···F−C, N−H···O, C−H···O, C−H···π_{HmtpO}, and N···π_{HmtpO} are also observed.[23,24,37,54] Thus, for example, there is intermolecular C−H···F hydrogen bonding between fluorine atoms of the fluorophenyl groups and hydrogen atoms of NBu_4^+ (F6···H50B contact of 2.285 Å, F8···H70B contact of 2.494 Å) and the intermolecular hydrogen bond interaction N4−H4···O11 (N···O11 contact of 2.724 Å). The H42···centroid (N2N3-C5N1C1) and N14···centroid (N2N3C5N1C1) distances are 2.959 Å and 2.863 Å, respectively.

Comparison Among the New Crystal Structures. In the Scheme 10 the metal−N3 bond distances of the seven new structures reported in this article are collected, together with the metal···metal distances of the dinuclear complexes.

The following observations can be found:

1. In the dinuclear complexes of the type $[NBu_4]_2[M(C_6F_5)_2(\mu\text{-mtpO})]_2$ [M = Pd (**11**·CH_2Cl_2·toluene) and Pt (**12**·0.5toluene)], the Pt−N3 distances are shorter than the Pd−N3. A similar observation has been previously found in other related systems, such as in $[NBu_4][M(C_6F_5)_2(pz)(Hpz)]$ (M = Pt, Pd; Hpz = pyrazole).[53]

2. The distance metal−N3 observed mainly depends on the nature of the donor atom in the trans position, rather than the neutral or anionic nature of the HmtpO/mtpO ligand, as illustrated in **7**·acetone and **14** (Scheme 10). On the other hand, the shorter metal−N3 distance is observed for **8**·$2H_2O$ (2.022 Å), where the mtpO ligand is trans to one of the N-donors of tmeda. Also, in **10a** two quite different Pd−N3 distances (2.077 and 2.175 Å) are observed, the longer corresponding to the mtpO ligand trans to the carbon donor of dmba, which possesses a higher trans influence.

3. The metal···metal separation in the dinuclear palladium **11**·CH_2Cl_2·toluene (3.560 Å) is longer than that observed in **10a** (3.0885 Å). This could be due to the long Pd−N distances observed in **11**·CH_2Cl_2·toluene, where the C_6F_5 ancillary is present (which possesses a great trans influence). Consequently, the dihedral angle of the coordination planes of the two metal atoms in **11**·CH_2Cl_2·toluene (50.72°) is higher than that found in **10a** (30.89°).

Biological Assays. Circular Dichroism Spectroscopy. The circular dichroism (CD) spectra of calf thymus DNA alone and incubated with the ligand HmtpO and its platinum(II) compounds **2** and **7** at 37 °C for 24 h with several molar ratios were recorded.

The free ligand HmtpO did not significantly modify either the ellipticity of the bands or their position. In contrast, the changes in ellipticity and wavelength caused by the new platinum(II) compounds **2** and **7** are significant (Figure 13). Both complexes reduce the ellipticity of the positive and negative bands with increasing values of r_i. An upshift in the λ_{max} (batochromic effect) is also observed. These results suggest modifications in the secondary structure of DNA caused by **2** and **7**, clearly indicating the transformation from DNA B form to DNA C form, with increasing winding of the DNA helix by rotation of the bases.[55–58]

Gel Electrophoresis of Compound-pB*R*322 Complexes. The influence of the compounds on the tertiary structure of DNA was determined by their ability to modify the electrophoretic mobility of the covalently closed circular (ccc) and open (oc) forms of pB*R*322 plasmid DNA. **2** and **7** and the HmtpO ligand were incubated at the molar ratio r_i = 0.50 with pB*R*322 plasmid DNA at 37 °C for 24 h. Representative gel obtained for the platinum complexes **2** and **7** are shown in Figure 14. The behavior of the gel electrophoretic mobility of both forms, ccc and oc, of pB*R*322 plasmid and DNA−cisplatin adducts is consistent with previous reports.[59] No changes were observed in sample incubated with the free ligand HmtpO. When the pB*R*322 was incubated with platinum compound **2** (lane 3), a single footprinting for both forms, ccc and oc, coalescent form, was observed. On the other hand, **7** (lane 4) accelerated the mobility of the ccc form.

The behavior observed for the electrophoretic mobility for the platinum complexes indicates that some conformational change occurred. This means that the degree of superhelicity of the DNA molecules has been altered. In contrast, the free ligand HmtpO does not seem to modify the tertiary structure of DNA.

(54) Hosmane, R. S.; Rossman, M. A.; Leonard, N. J. *J. Am. Chem. Soc.* **1982**, *104*, 5497–5499.
(55) Macquet, J. P.; Butour, J. L. *Biochimie* **1978**, *60*, 901–914.
(56) Brabec, V.; Kleinwächter, V.; Butour, J.; Johnson, M. P. *Biophys. Chem.* **1990**, *35*, 129–141.
(57) Cervantes, G.; Prieto, M. J.; Moreno, V. *Metal Based Drugs* **1997**, *4*, 9.
(58) Cervantes, G.; Marchal, S.; Prieto, M. J.; Pérez, J. M.; González, V. M.; Alonso, C.; Moreno, V. *J. Inorg. Biochem.* **1999**, *77*, 197–203.
(59) Ushay, H. M.; Tullius, T. D.; Lippard, S. J. *Biochemistry* **1981**, *20*, 3744–3748.

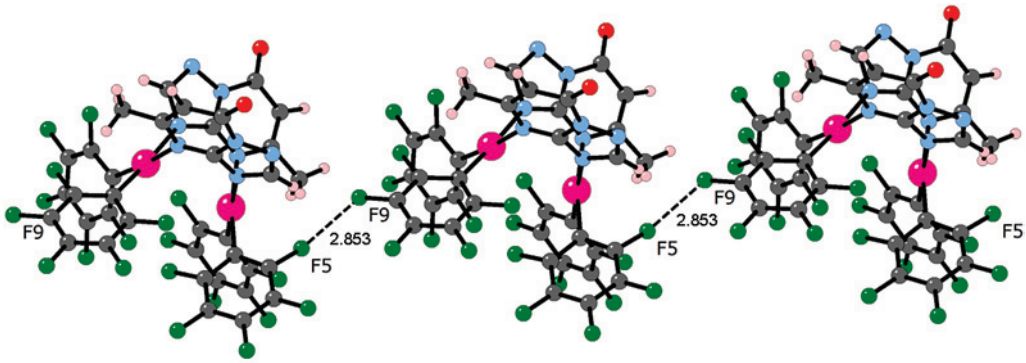

Figure 10. Schematic showing the chain formed by F5···F9 contact in **12**·0.5(toluene).

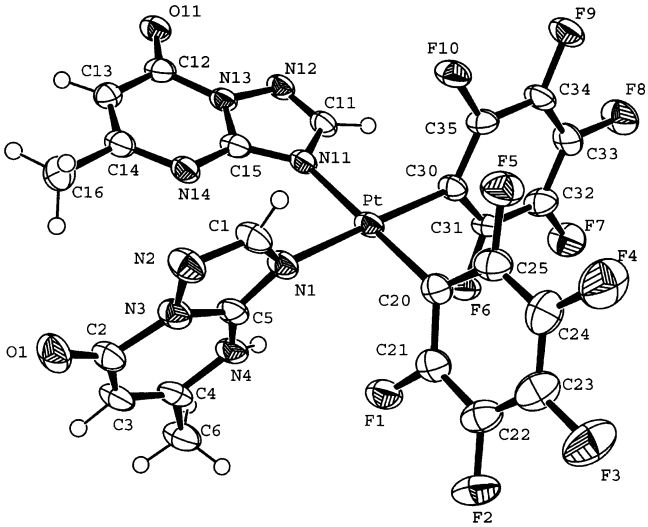

Figure 11. ORTEP representation (50% probability) of **14**. Selected bond lengths (Å) and angles (deg): Pt(1)−C(20) = 1.995(5), Pt(1)−C(30) = 2.005(4), Pt(1)−N(1) = 2.072(4), Pt(1)−N(11) = 2.096(4), C(20)−Pt(1)−N(30) = 87.87(18), C(20)−Pt(1)−N(1) = 89.43(16), C(30)−Pt(1)−N(1) = 176.50(16), C(20)−Pt(1)−N(11) = 179.14(16), C(30)−Pt(1)−N(11) = 91.77(16), N(1)−Pt(1)−N(11) = 90.95(14).

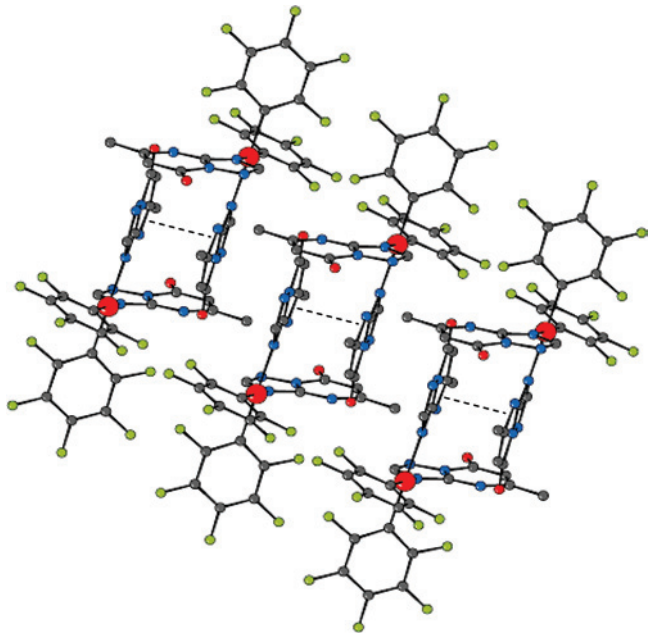

Figure 12. π-stacking interactions between nitrogen aromatic rings. One molecule establishes π-stacking interactions with another related by symmetry operation through $-x, -y, -z + 2$.

AFM Study of Compound-pB*R*322 Complexes. Consequently to the behavior observed in the electrophoretic mobility, the platinum complexes **2** and **7** modify the morphology of the pB*R*322 DNA, and the ccc forms are predominant in the pictures (Figure 15). In all cases, the complexes seem to modify the morphology of the pB*R*322 DNA in similar mode as cisplatin does.[17,57–61] The platinum complexes attached to DNA cause kinks and cross-linking in the plasmid forms. The background of part b of Figure 15 indicates the presence of a layer of water molecules from the environment over the mica surface, which can be the origin of the aggregation of the forms.

Cytotoxicity Studies. The in vitro growth inhibitory effect of **2** and **7** and cisplatin was evaluated in a panel of human tumor cell lines representative of ovarian (A2780 and A2780cisR), lung (NCI-H460, nonsmall lung cancer cell), and breast cancers (T47D, cisplatin resistant). A2780cisR encompasses all of the known major mechanisms of resistance to cisplatin: reduced drug transport,[62] enhanced DNA repair/tolerance,[63] and elevated GSH levels.[64] Table 2 shows the IC_{50} values and the resistance factors (RF) of the new platinum complexes. The ability of **2** and **7** to circumvent cisplatin-acquired resistance was determined from the RF, defined as the ratio of the IC_{50} resistant line to the IC_{50} parent line. An RF of <2 was considered to denote noncross-resistance.[65] Especially noteworthy are the very low RFs of both complexes at 48 h (RF = 1.4 and 1.2, respectively), indicating efficient circumvention of cisplatin resistance (Table 3).

On the other hand, a 48 h incubation time for **2** and **7** were about 8-fold more active than cisplatin in T47D,

(60) Onoa, G. B.; Cervantes, G.; Moreno, V.; Prieto, M. J. *Nucleic Acids Res.* **1998**, *26*, 1473–1480.
(61) Onoa, G. B.; Moreno, V. *Int. J. Pharm.* **2002**, *245*, 55–65.
(62) Loh, S. Y.; Mistry, P.; Kelland, L. R.; Abel, G.; Harrap, K. R. *Br. J. Cancer* **1992**, *66*, 1109–1115.
(63) Goddard, P. M; Orr, R. M.; Valenti, M. R.; Barnard, C. F.; Murrer, B. A.; Kelland, L. R.; Harrap, K. R. *Anticancer Res.* **1996**, *16*, 33–8.
(64) Behrens, B. C.; Hamilton, T. C.; Masuda, H.; Grotzinger, K. R.; Whang-Peng, J.; Louie, K. G.; Knutsen, T.; McKoy, W. M.; Young, R. C.; Ozols, R. F. *Cancer Res.* **1987**, *47*, 414–418.
(65) Kelland, L. R.; Barnard, C. F. J.; Mellish, K. J.; Jones, M.; Goddard, P. M.; Valenti, M.; Bryant, A.; Murrer, B. A.; Harrap, K. R. *Cancer Res.* **1994**, *54*, 5618–5622.

Scheme 10

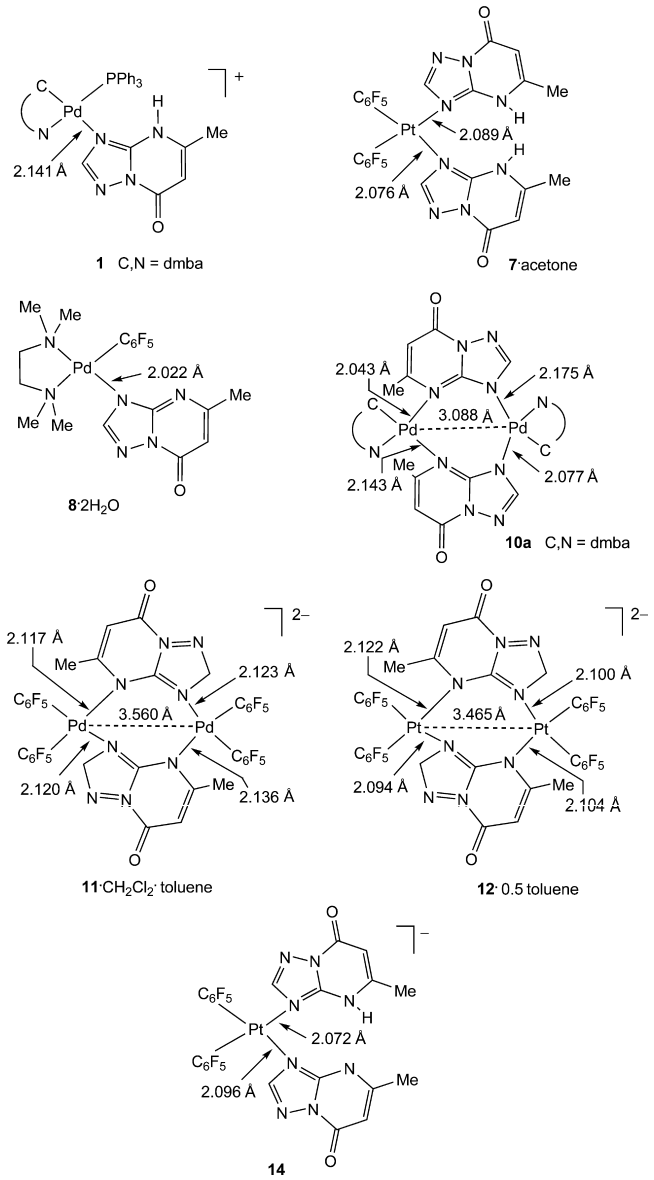

whereas in NCI-H460 similar values of IC_{50} than cisplatin were obtained.

Experimental Section

Instrumental Measurements. The carbon, hydrogen, and nitrogen analyses were performed with a Carlo Erba model EA 1108 microanalyzer. Decomposition temperatures were determined with a SDT 2960 simultaneous DSC-TGA of TA instruments at a heating rate of 5 °C min^{-1} and the solid samples under nitrogen flow (100 mL min^{-1}). The ^1H, ^{13}C, ^{31}P, and ^{19}F NMR spectra were recorded on a Bruker AC 200E or Bruker AC 300E spectrometer, using $SiMe_4$, H_3PO_4, and $CFCl_3$ as standards. Infrared spectra were recorded on a PerkinElmer 1430 spectrophotometer using Nujol mulls between polyethylene sheets. Mass spectra (positive-ion FAB) were recorded on a V.G. AutoSpecE spectrometer and measured using 3-nitrobenzyl alcohol as the dispersing matrix.

Materials. The starting complexes $[M(dmba)Cl(PPh_3)]$ (M = Pd or Pt),[10,11] $[Pd(N-N)(C_6F_5)Cl)]$ (N−N = bpy, Me_2bpy, or tmeda),[66] $[NBu_4]_2[Pd_2(C_6F_5)_4(\mu\text{-}Cl)_2]$,[31] *cis*-$[Pt(C_6F_5)_2(THF)_2]$,[32] $[Pd(N-N)(C_6F_5)(OH)]$ (N−N = tmeda),[28] $[Pd(dmba)(\mu\text{-}OH)]_2$,[14] and $[NBu_4]_2[M_2(C_6F_5)_4(\mu\text{-}OH)_2]$ (M = Pd or Pt)[51,52] were prepared by procedures described elsewhere. Solvents were dried by the usual methods. 4,7-dihydro-5-methyl-7-oxo[1,2,4]triazolo[1,5-a]pyrimidine (HmtpO), sodium salt of calf thymus DNA, EDTA (ethylene diaminotetracetic acid), and Tris-HCl (tris-(hydroxymethyl)aminomethane-hydrochloride) used in the circular dichroism (CD) study were obtained from Sigma-Aldrich (Madrid, Spain), HEPES (*N*-2-hydroxyethyl piperazyne-*N*′-2-ethanesulfonic acid) was obtained from ICN (Madrid), and pB*R*322 plasmid DNA was obtained from Boehringer-Mannheim (Mannheim, Germany).

Warning! *Perchlorate salts of metal complexes with organic ligands are potentially explosive. Only small amounts of material should be prepared, and these should be handled with great caution.*

Preparation of $[Pd(dmba)(PPh_3)(HmtpO)]ClO_4$ 1. To a solution of $[Pd(dmba)(Cl)(PPh_3)]$ (0.185 mmol, 100 mg) in CH_2Cl_2 (20 mL) was added $AgClO_4$ (0.185 mmol, 38.5.0 mg). AgCl immediately formed. The resulting suspension was stirred for 30 min and then filtered through a short pad of Celite. To the filtrate was then added HmtpO (0.185 mmol, 27.8 mg). The solution was stirred for 5 h, and then the solvent was partially evaporated under vacuum and hexane added to precipitate a white solid, which was collected by filtration and air-dried.

Data for 1. Yield: 65%. Anal. Calcd for $C_{33}H_{33}ClN_5O_5PPd$: C, 52.7; H, 4.4; N, 9.3. Found: C, 52.4; H, 4.4; N, 9.1. Mp: 230 °C dec Λ_M: 135 S cm^2 mol^{-1}. IR (Nujol, cm^{-1}): ν(CO), 1716; ClO_4, 1095, 623. ^1H NMR ($CDCl_3$): δ ($SiMe_4$) 11.53 (s, 1H, NH of HmtpO), 7.92 (s 1H, H2 of HmtpO), 7.68 (m, 6H, P*Ph*$_3$), 7.37 (m, 9H, P*Ph*$_3$), 7.03 (d, 1H, C_6H_4, J_{HH} = 7.6 Hz), 6.86 (false t, 1H, C_6H_4, $J_{HH} \approx J_{HH}$ = 8.2 Hz), 6.35 (m, 2H, C_6H_4), 5.69 (s, 1H, H6 of HmtpO), 5.29 (br, 1H, NCH_2 of dmba), 3.46 (br, 1H, NCH_2 of dmba), 2.71 (br, 3H, N*Me*$_2$ of dmba), 2.58 (br, 3H, N*Me*$_2$ of dmba), 2.40 (s, 3H, *Me* of HmtpO). ^{31}P NMR ($CDCl_3$): δ (H_3PO_4) 41.78 (s).

Preparation of $[Pt(dmba)(PPh_3)(HmtpO)]ClO_4$ 2. To a solution of $[Pt(dmba)(PPh_3)Cl]$ (0.159 mmol, 100 mg) in acetone (20 mL) was added $AgClO_4$ (0.159 mmol, 33.1 mg). AgCl immediately formed. The resulting suspension was stirred for 30 min and then filtered through a short pad of Celite. To the filtrate was then added HmtpO (0.159 mmol, 23.9 mg). The resulting solution was stirred for 5 h, and then the solvent was partially evaporated under vacuum. A white solid obtained which was collected by filtration and air-dried.

Data for 2. Yield: 88%. Anal. Calcd for $C_{33}H_{33}ClN_5O_5PPt$: C, 47.1; H, 4.0; N, 8.3. Found: C, 47.3; H, 3.9; N, 8.4. Mp: 269 °C dec Λ_M: 150 S cm^2 mol^{-1}. IR (Nujol, cm^{-1}): ν(CO), 1715; ClO_4, 1095, 623. ^1H NMR ($CDCl_3$): δ ($SiMe_4$) 11.63 (s, 1H, NH of HmtpO), 7.92 (s 1H, H2 of HmtpO), 7.69 (m, 6H, P*Ph*$_3$), 7.33 (m, 9H, P*Ph*$_3$), 7.08 (d, 1H, C_6H_4, J_{HH} = 7.1 Hz), 6.88 (false t, 1H, C_6H_4, $J_{HH} \approx J_{HH}$ = 7.2), 6.38 (m, 2H, C_6H_4), 5.69 (s, 1H, H6 of HmtpO), 5.17 (d, 1H, NCH_2 of dmba, J_{HH} = 13.0 Hz), 3.70 (dd, 1H, NCH_2 of dmba, J_{HH} = 13.2, J_{HP} = 2.5 Hz), 2.78 (s, 3H, N*Me*$_2$ of dmba), 2.74 (s, 3H, N*Me*$_2$ of dmba), 2.45 (s, 3H, *Me* of HmtpO). ^{31}P NMR ($CDCl_3$): δ (H_3PO_4) 19.30 (J_{PtP} = 4136 Hz).

Preparation of $[Pd(N-N)(C_6F_5)(HmtpO)]ClO_4$ 3−5. To a solution of $[Pd(N-N)(C_6F_5)(Cl)]$ (0.214 mmol) [N−N = bpy (2,2′-bipyridyl), Me_2bpy (4,4′-dimethyl-2,2′-bipyridyl) or *N*,*N*,*N*′,*N*′-tmeda (tetramethylethylenediamine)] in acetone (20 mL) was added $AgClO_4$ (0.214 mmol, 44.5 mg). AgCl immediately formed. The resulting suspension was stirred for 30 min and then filtered through a short pad of Celite. To the filtrate was then added HmtpO (0.214 mmol, 32.2 mg). The resulting solution was stirred for 5 h, and then the solvent was partially evaporated under vacuum. A white solid obtained, which was collected by filtration and air-dried.

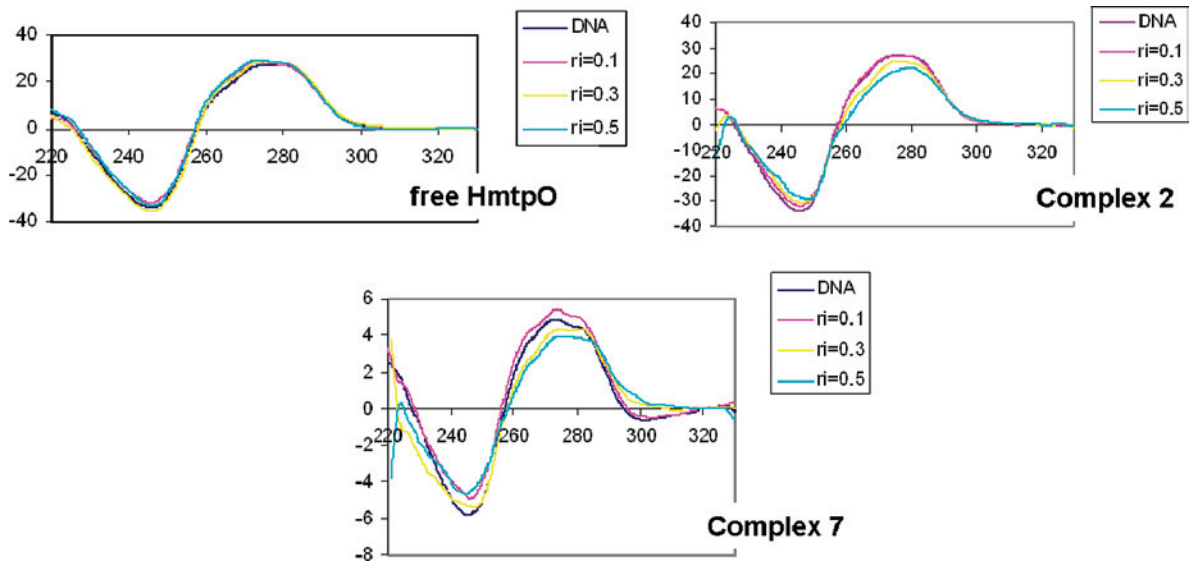

Figure 13. Circular dichroism spectra of DNA and DNA incubated with free HmtpO, **2**, and **7** at different r_i.

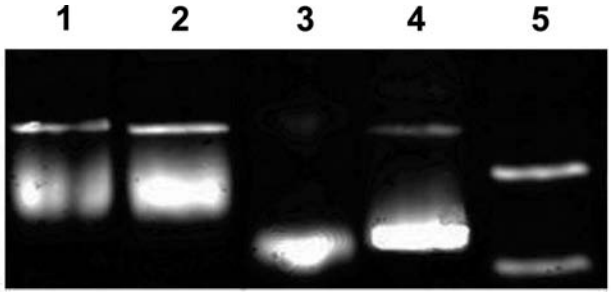

Figure 14. Modification of the gel electrophoretic mobility of pB*R*322 plasmid incubated with HmtpO and their platinum compounds: lane 1, pBR; lane 2, HmtpO; lane 3, **2**; lane 4, **7**; lane 5, pBR−cisplatin.

Data for 3. Yield: 65%. Anal. Calcd for $C_{22}H_{14}ClF_{56}O_5Pd$: C, 38.9; H, 2.1; N, 12.4. Found: C, 38.6; H, 2.2; N, 12.5. Mp: 251 °C dec Λ_M: 144 S cm^2 mol^{-1}. IR (Nujol, cm^{-1}): ν(CO), 1710; ν(Pd−C_6F_5), 772. ^{1}H NMR (acetone-d_6): δ(SiMe$_4$) 12.81 (s, 1H, NH of HmtpO), 8.74 (m, 2H, $H_\alpha + H_{\alpha'}$ of bpy), 8.45 (m, 2H, $H_\gamma + H_{\gamma'}$ of bpy), 8.46 (s, 1H, H2 of HmtpO), 8.34 (d, 1H, H_δ or $H_{\delta'}$ of bpy, $J_{HH} = 5.6$ Hz), 8,18 (d, 1H, H_δ or $H_{\delta'}$ of bpy, $J_{HH} = 5.4$ Hz), 7.70 (m, 2H, $H_\beta + H_{\beta'}$ of bpy), 6.07 (s, 1H, H6 of HmtpO), 2.83 (s, 3H, Me of HmtpO). ^{19}F NMR (acetone-d$_6$): δ(CFCl$_3$) −120.35 (m, 1F$_o$), −121.25 (m, 1F$_o$), −160.73 (t, 1F$_p$, $J_{FpFm} =$ 18.8 Hz), −163.41 (m, 2F$_m$).

Data for 4. Yield: 72%. Anal. Calcd for $C_{24}H_{18}ClF_5N_6O_5Pd$: C, 40.8; H, 2.6; N, 11.9. Found: C, 40.5; H, 2.6; N, 12.1. Mp: 260 °C dec Λ_M: 142 S cm^2 mol^{-1}. IR (Nujol, cm^{-1}): ν(CO), 1720; ν(Pd−C_6F_5), 796. ^{1}H NMR (acetone-d_6): δ (SiMe$_4$) 12.59 (s, 1H, NH of HmtpO), 8.04 (s, 1H, H2 of HmtpO), 7.95 (s, 2H, $H_\delta + H_{\delta'}$ of Me$_2$bpy), 7.62 (d, 1H, H_α of Me$_2$bpy, $J_{H\alpha H\beta} = 6.0$ Hz), 7.41 (d, 1H, $H_{\alpha'}$ of Me$_2$bpy, $J_{H\alpha' H\beta'} = 5.7$ Hz), 7.25 (d, 1H, H_β of Me$_2$bpy, $J_{H\alpha H\beta} = 6.0$ Hz), 7.18 (d, 1H, $H_{\beta'}$ of Me$_2$bpy, $J_{H\alpha' H\beta'} = 5.7$ Hz), 5.99 (s, 1H, H6 of HmtpO), 2.58 (s, 3H, Me of HmtpO), 2,54 (s, 6H, Me of Me$_2$bpy). ^{19}F NMR (acetone-d_6): δ (CFCl$_3$) −118.29 (m, 1F$_o$), −120.50 (m, 1F$_o$), −155.96 (t, 1F$_p$, J_{FpFm} 20.1 Hz), −159.14 (m, 1F$_m$), −159.97 (m, 1F$_m$).

Data for 5. Yield: 55%. Anal. Calcd for $C_{18}H_{22}ClF_5N_6O_5Pd$: C, 33.8; H, 3.5; N, 13.2. Found: C, 33.6; H, 3.8; N, 12.9. Mp: 236 °C dec Λ_M: 130 S cm^2 mol^{-1}. IR (Nujol, cm^{-1}): ν(CO), 1730; ν(Pd−C_6F_5), 790. ^{1}H NMR (acetone-d_6): δ (SiMe$_4$) 11.85 (s, 1H, NH of HmtpO), 8.37 (s, 1H, H2 of HmtpO), 5.96 (s, H, H6 of HmtpO), 3.28 (m, 4H, CH$_2$ of tmeda), 2.75 (m, 12H, NMe$_2$ of tmeda), 2.55 (s, 3H, Me of HmtpO). ^{19}F NMR (acetone-d_6): δ (CFCl$_3$) −120.18 (m, 1F$_o$), −121.93 (m, 1F$_o$), −161.56 (t, 1F$_p$, J_{FpFm} 18.8 Hz), −163.57 (m, 1F$_m$), −164.47 (m, 1F$_m$).

Preparation of *cis*-[Pd(C_6F_5)$_2$(HmtpO)$_2$] 6. To a solution of [NBu$_4$]$_2$[Pd$_2$(C_6F_5)$_4$(μ-Cl)$_2$] (100 mg, 0.070 mmol) in acetone (20 mL) was added AgClO$_4$ (28.9 mg, 0.140 mmol). AgCl inmediately formed. The resulting suspension was stirred for 30 min and then filtered through a short pad of Celite. To the filtrate was then added HmtpO (41.8 mg, 0.278 mmol). The solution was stirred for 24 h, then the solvent was partially evaporated under vacuum, and hexane was added to precipitate a white solid, which was collected by filtration and air-dried.

Data for 6. Yield: 55%. Anal. Calcd for $C_{24}H_{12}F_{10}N_8O_2Pd$: C, 38.9; H, 1.6; N, 15.1. Found: C, 38.8; H, 1.8; N, 15.2. Mp: 175 °C dec IR (Nujol, cm^{-1}): ν(CO), 1713, 1694; ν(Pd−C_6F_5), 798, 787. ^{1}H NMR acetone-d_6, −50 °C): δ (SiMe$_4$) 13.0 (s, 2H, NH of HmtpO), 8.65 (s, 2H, H2 of HmtpO), 5.96 (s, 2H, H6 of HmtpO), 2.42 (s, 6H, CMe of HmtpO). ^{19}F NMR (acetone-d_6): δ (CFCl$_3$) −115.90 (m, 4F$_o$), −162.69 (t, 2F$_p$, J_{FpFm} 18.8 Hz), −165.04 (m, 4F$_m$).

Preparation of *cis*-[Pt(C_6F_5)$_2$(HmtpO)$_2$] 7. To a solution of *cis*-[Pt(C_6F_5)$_2$(THF)$_2$] (145 mg, 0.215 mmol) in acetone (20 mL) was added HmtpO (64.6 mg, 0.43 mmol). The solution was stirred for 20 h. The solvent was evaporated off under reduced pressure. The residue was treated with diethyl ether to render a white solid, which was collected by filtration and air-dried.

Data for 7. Yield: 55%. Anal. Calcd for $C_{22}H_{12}F_{10}N_8O_2Pt$: C, 32.8; H, 1.5; N, 13.9. Found: C, 33.0; H, 1.5; N, 13.6. Mp: 250 °C dec IR (Nujol, cm^{-1}): ν(CO), 1713, 1682; ν(Pt−C_6F_5), 810, 801. ^{1}H NMR (acetone-d_6): δ (SiMe$_4$) 12.37 (s, 2H, NH of HmtpO), 8.60 (s, 2H, H2 of HmtpO), 5.89 (s, 2H, H6 of HmtpO), 2.48 (s, 6H, Me of HmtpO). ^{19}F NMR (acetone-d_6): δ (CFCl$_3$) −120.58 (m, 4F$_o$), −165.40 (t, 2F$_p$, J_{FpFm} 16.9 Hz), −167.32 (m, 4F$_m$).

Preparation of [Pd(tmeda)(C_6F_5)(mtpO)] 8. To a solution of [Pd(tmeda)(C_6F_5)(OH)] (100 mg, 0.245 mmol) in methanol (20 mL) was added HmtpO (36.8 mg, 0.245 mmol). The resulting mixture was stirred for 1 h at room temperature, during which time the white mononuclear complex precipitated, and then the solvent was partly evaporated under reduced pressure. The complex was filtered off and air-dried.

Data for 8. Yield: 60%. Anal. Calcd for $C_{18}H_{21}F_5N_6OPd$: C, 40.1; H, 3.9; N, 15.6. Found: C, 40.2; H, 3.9; N, 15.5. Mp: 240 °C

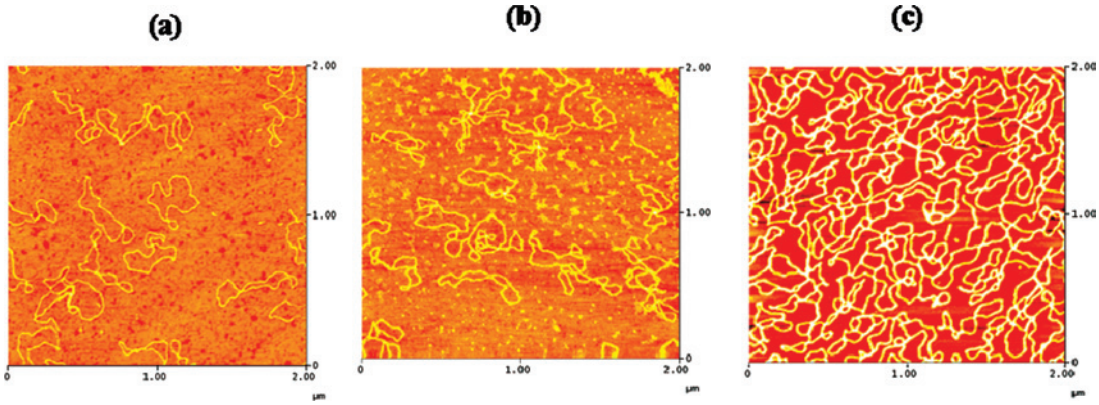

Figure 15. TMAFM image corresponding to (a) pB*R*322, (b) pBR−**2**, and (c) pBR−**7**.

Table 3. IC_{50} (μM) and resistance factors for Cisplatin and Complexes **2** and **7**

	T47D		NCI-H460		A2780		A2780cisR	
complex	24 h	48 h	24 h	48 h	24 h	48 h	24 h (RF)[a]	48 h (RF)[a]
2	55.5	4.7	7.0	9.0	3.9	3.9	6.2 (1.6)	5.3 (1.4)
7	30.5	4.6	12.0	9.0	5.4	7.1	10 (1.9)	8.8 (1.2)
cisplatin	34.0	35.0	6.0	9.0	10.0	0.98	17 (1.7)	18 (18.4)

[a] The numbers in parentheses are the resistance factors RF (IC_{50} resistant/IC_{50} sensitive).

dec IR (Nujol, cm^{-1}): ν(CO), 1660; ν(Pd−C_6F_5), 770. ^{1}H NMR ($CDCl_3$): δ ($SiMe_4$) 7.75 (s, 1H, H2 of mtpO), 5.83 (s, 1H, H6 de mtpO), 2.86 (br, 2H, CH_2 of tmeda), 2.83 (br, 2H, CH_2 of tmeda), 2.68 (s, 6H, NMe_2 of tmeda), 2.62 (s, 6H, NMe_2 of tmeda), 2.35 (s, 3H, Me of mtpO). ^{19}F NMR ($CDCl_3$): δ ($CFCl_3$) −121.65 (m, $2F_o$), −158.29 (t, $1F_p$, J_{FpFm} 28,8), −161.59 (m, $2F_m$).

Preparation of [Pd(dmba)(PPh$_3$)(mtpO)] 9. To a solution of [Pd(dmba)(μ-OH)]$_2$(100 mg, 0.195 mmol) in CH_2Cl_2 (20 mL) was added PPh_3 (102.3 mg, 0.390 mmol) and HmtpO (58.6 mg, 0.390 mmol). The resulting mixture was stirred for 1 h at room temperature, and then the solvent was partially evaporated under vacuum, and hexane was added to precipitate a white solid, which was collected by filtration and air-dried.

Data for 9. Yield: 98%. Anal. Calcd for $C_{33}H_{32}N_5OPPd$: C, 60.8; H, 5.0; N, 10.7. Found: C, 60.6; H, 4.9; N, 10.9. Mp: 246 °C dec IR (Nujol, cm^{-1}): ν(CO), 1660. ^{1}H NMR ($CDCl_3$): δ ($SiMe_4$) 7.61 (m, 7H, H2 of HmtpO + P*Ph*$_3$), 7.31(m, 9H, P*Ph*$_3$), 7.04 (d, 1H, C_6H_4, J_{HH} = 7.4 Hz), 6.86 (false t, 1H, C_6H_4, $J_{HH} \approx J_{H-H}$ = 8.2 Hz), 6.41 (m, 2H, C_6H_4), 5.58 (br, 1H, H6 of mtpO), 4.22 (br, 1H, NC*H*$_2$ of dmba), 4.07 (br, 1H, NC*H*$_2$ of dmba), 2.64 (br, 6H, N*Me*$_2$), 2.25 (s, 3H, *Me* of mtpO). ^{31}P NMR ($CDCl_3$): δ (H_3PO_4) 43.31 (s).

Preparation of Dimeric Palladium Complexes [Pd(dmba)(μ-mtpO)]$_2$ 10a and 10b. To a solution of [Pd(dmba)(μ-OH)]$_2$ (100 mg, 0.195 mmol) in methanol (15 mL) was added HmtpO (58.6 mg, 0.390 mmol). The resulting mixture was stirred for 20 min at room temperature, and then the solvent was partially evaporated under vacuum, and a suspension was obtained from which a white solid was collected by filtration and air-dried. Accordingly, with the ^{1}H NMR in $CDCl_3$ two linkage isomers (**10a** and **10b**) are present in a ratio (1:0.4). The H−H isomer **10a** was isolated pure by crystallization in CH_2Cl_2/toluene/hexane of the mixture, whereas the H−L isomer **10b** was isolated pure by washing the mixture with ethanol.

Data for 10a. Yield: 35%. Anal. Calcd for $C_{30}H_{34}N_{10}O_2Pd_2$: C, 46.2; H, 4.4; N, 18.0. Found: C, 46.1; H, 4.5; N, 17.9. Mp: 265 °C dec IR (Nujol, cm^{-1}): ν(CO), 1680. ^{1}H NMR ($CDCl_3$): δ ($SiMe_4$) 8.41 (s, 1H, H2 of mtpO), 7.89 (s, 1H, H2 of mtpO), 7.05 (m, 2H, C_6H_4), 6.91 (m, 5H, C_6H_4), 6.68 (d, 1H, C_6H_4, J_{HH} = 6.8 Hz), 6.17 (s, 1H, H6 of mtpO), 5.91 (s, 1H, H6 of mtpO), 3.29 (d, 1H, NC*H*$_2$, J_{HH} = 13.0 Hz), 2.93 (d, 1H, NC*H*$_2$, J_{HH} = 13.0 Hz), 2.92 (d, 1H, NC*H*$_2$, J_{HH} = 13.6 Hz), 3.16 (s, 3H, Me of mtpO), 2.99 (s, 3H, NMe_2), 2.96 (s, 3H, NMe_2), 2.73 (d, 1H, NC*H*$_2$, J_{HH} = 13.6 Hz), 2.67 (s, 3H, Me of mtpO), 1.817 (s, 3H, NMe_2), 1.61 (s, 3H, NMe_2).

Data for 10b. Yield: 17%. Anal. Calcd for $C_{30}H_{34}N_{10}O_2Pd_2$: C, 46.2; H, 4.4; N, 18.0. Found: C, 46.0; H, 4.6; N, 17.8. Mp: 272 °C dec ^{1}H NMR ($CDCl_3$): δ ($SiMe_4$) 8.44 (s, 2H, H2 of mtpO), 7.07 (m, 2H, C_6H_4), 6.95 (m, 4H, C_6H_4), 6.84 (d, 2H, C_6H_4, J_{HH} = 7.4 Hz), 5.89 (s, 2H, H6 de mtpO), 2.83 (s, 4H, NC*H*$_2$), 2.76 (s, 6H, NMe_2), 3.19 (s, 6H, Me of mtpO), 1.79 (s, 6H, NMe_2).

Preparation of [NBu$_4$]$_2$[M(C$_6$F$_5$)$_2$(μ-mtpO)]$_2$ (11 and 12) and [NBu$_4$][M(C$_6$F$_5$)$_2$(mtpO)(HmtpO)] (13 and 14) (M = Pd or Pt). To a solution of [NBu$_4$]$_2$[M(C$_6$F$_5$)$_2$(μ-OH)]$_2$ (M = Pd or Pt) (0.071 mmol) in acetone (20 mL) was added HmtpO (21.4 mg, 0.142 mmol). The suspension was stirred for 24 h at room temperature. The resulting solution was concentrated under vacuum to dryness. Addition of ether yielded a white solid which was filtered off and air-dried. The isolated solids were identified by NMR spectroscopy as a mixture containing the corresponding [NBu$_4$]$_2$-[M(C$_6$F$_5$)$_2$(μ-mtpO)]$_2$ (**11** or **12**) and [NBu$_4$][M(C$_6$F$_5$)$_2$(mtpO)-(HmtpO)] (**13** or **14**) in a molar ratio of approximately 1:0.4, together with starting material. The platinum complexes **12** and **14** were separated mechanically after crystallization from dichloromethane/toluene/hexane. In the case of palladium, only crystals of **11** could be obtained.

Data for 11. Yield: 16%. Anal. Calcd for $C_{68}H_{83}F_{20}N_{10}O_2Pd_2$: C, 49.1; H, 5.0; N, 8.4. Found: C, 49.0; H, 4.8; N, 8.3. ^{1}H NMR ($CDCl_3$): δ ($SiMe_4$) 8.44 (s, 2H, H2 of mtpO), 5.43 (s, 2H, H6 of mtpO), 3.44 (m, 16H, C*H*$_2$N of NBu$_4$), 2.87 (s, 6H, Me of mtpO), 2.04 (m, 16H, C*H*$_2$ of NBu$_4$), 1.40 (m, 16H, C*H*$_2$ of NBu$_4$), 0.93 (t, 24H, Me de NBu$_4$, J_{HH} 7.4), ^{19}F NMR ($CDCl_3$): δ ($CFCl_3$) −112.44 (m, $8F_o$), −165.40 (t, $2F_p$, J_{FpFm} = 20.7 Hz), −165.80 (t, $2F_p$, J_{FpFm} = 20.7 Hz), −167.16 (m, $4F_m$), −167.68 (m, $4F_m$).

Data for 12. Yield: 14%. Anal. Calcd for $C_{68}H_{83}F_{20}N_{10}O_2Pt_2$: C, 44.3; H, 4.5; N, 7.6. Found: C, 44.6; H, 4.3; N, 7.8. ^{1}H NMR ($CDCl_3$): 8.67 (s, 2H, H2 of mtpO), 5.59 (s, 2H, H6 of mtpO), 3.09 (m, 16H, C*H*$_2$N of NBu$_4$), 2.80 (s, 6H, Me of mtpO), 1.40 (m, 16H, C*H*$_2$ of NBu$_4$), 1.25 (m, 16H, C*H*$_2$ of NBu$_4$), 0.86 (t, 24H, Me of NBu$_4$), ^{19}F NMR ($CDCl_3$): δ ($CFCl_3$) −117.14 (m, $8F_o$, J_{PtFo} = 406 Hz), −165.62 (t, $2F_p$, J_{FpFm} = 19.7 Hz), −165.97 (m, 2Fp, J_{FpFm} = 19.7 Hz), −167.30 (m, $4F_m$), −168.14 (m, $4F_m$).

Data for 13. ^{1}H NMR ($CDCl_3$): 7.94 (s, 2H, H2 of mtpO), 6.01 (s, 2H, H6 of mtpO), 3.44 (m, 8H, C*H*$_2$N of NBu$_4$), 2.41 (s, 6H, Me of mtpO), 2.05 (m, 8H, C*H*$_2$ of NBu$_4$), 1.41 (m, 8H, C*H*$_2$ of NBu$_4$), 0.95 (t, 12H, Me de NBu$_4$, J_{HH} 7.4), ^{19}F NMR ($CDCl_3$): δ

Table 4. Crystal Structure Determination Details of **1**, **7**·acetone, **8**·$2H_2O$ and **10a**

params	**1**	**7**·acetone	**8**·$2H_2O$	**10a**
empirical formula	$C_{33}H_{33}ClN_5O_5PPd$	$C_{27}H_{18}F_{10}N_8O_3Pt$	$C_{18}H_{25}F_5N_6O_3Pd$	$C_{30}H_{34}N_{10}O_2Pd_2$
fw	752.46	887.58	574.84	779.47
cryst syst	monoclinic	monoclinic	triclinic	monoclinic
a (Å)	11.7034(5)	14.1739(6)	9.2868(8)	9.7961(8)
b (Å)	36.114(2)	15.8664(6)	10.5789(6)	27.5078(18)
c (Å)	9.5959(6)	13.3379(5)	12.4126(7)	11.3078(8)
α (deg)	90	90	82.845(4)	90
β (deg)	125.764(4)	99.899(2)	78.512(6)	96.253(6)
γ (deg)	90	90	69.745(6)	90
V (Å^3)	3291.0(3)	2954.9(2)	1119.08(13)	3029.0(4)
T (K)	173(2)	100(2)	173(2)	173(2)
space group	Cc	$P2_1/c$	P-1	$P2_1/n$
Z	4	4	2	4
μ (mm^{-1})	0.742	4.859	0.903	1.234
reflns collected	5783	33115	7918	6040
independent reflns	5150	6830	3938	5333
R(int)	0.0237	0.0521	0.0207	0.0280
R1 [$I > 2\sigma$ (I)][a]	0.0264	0.0366	0.0242	0.0334
wR_2 (all data)[b]	0.0676	0.0698	0.0620	0.0760

[a] R1 $=\sum||F_o| - |F_c||/\sum|F_o|$, wR2 $= [\sum[w(F_o^2 - F_c^2)^2]/\sum w(F_o^2)^2]^{0.5}$. [b] $w = 1/[\sigma^2(F_o^2) + (aP)^2 + bP]$, where $P = (2F_c^2 + F_o^2)/3$ and a and b are constants set by the program.

Table 5. Crystal Structure Determination Details of **11**·CH_2Cl_2·toluene, **12**·0.5(toluene) and **14**

params	**11**·CH_2Cl_2·toluene	**12**·0.5(toluene)	**14**
empirical formula	$C_{78}H_{92}Cl_2F_{20}N_8O_2Pd_2$	$C_{71.50}H_{86}F_{20}N_{10}O_2Pt_2$	$C_{40}H_{47}F_{10}N_9O_2Pt$
fw	1837.30	1887.68	1070.96
cryst syst	triclinic	monoclinic	monoclinic
a (Å)	15.2953(7)	12.4458(5)	10.4660(4)
b (Å)	17.0706(8)	46.806(2)	20.5620(8)
c (Å)	17.9758(8)	14.2160(6)	21.5847(8)
α (deg)	95.718(2)	90	90
β (deg)	108.812(2)	113.605(2)	93.0840(10)
γ (deg)	110.224(2)	90	90
V(Å^3)	4049.4(3)	7588.4(6)	4638.3(3)
T (K)	100(2)	100(2)	100(2)
space group	P-1	$P2_1/n$	$P2_1/n$
Z	2	4	4
μ (mm^{-1})	0.607	5.182	3.109
reflns collected	44 817	87 941	50 823
independent reflns	16 452	17 770	9478
R(int)	0.0186	0.0640	0.0538
R1 [$I > 2\sigma$ (I)][a]	0.0463	0.0482	0.0402
wR_2 (all data)[b]	0.1377	0.0922	0.0972

[a] R1 $=\sum||F_o| - |F_c||/\sum|F_o|$, wR2 $= [\sum[w(F_o^2 - F_c^2)^2]/\sum w(F_o^2)^2]^{0.5}$. [b] $w = 1/[\sigma^2(F_o^2) + (aP)^2 + bP]$, where $P(2F_c^2 + F_o^2)/3$, and a and b are constants set by the program.

($CFCl_3$) −115.16 (m, $2F_o$), −115.79 (m, $2F_o$), −164.2 (t, $2F_p$, J_{FpFm} = 22.6), −166.4 (m, $4F_m$).

Data for 14. Yield: 10%. Anal. Calcd for $C_{41}H_{50}F_{10}N_9O_2Pt$: C, 45.4; H, 4.6; N, 11.6. Found: C, 45.8; H, 4.3; N, 11.7. ^{1}H NMR ($CDCl_3$): 8.06 (s, 2H, H2 of mtpO), 5.74 (s, 2H, H6 of mtpO), 3.15 (m, 8H, CH_2N of NBu_4), 2.38 (s, 6H, Me of mtpO), 1.66 (m, 8H, CH_2 of NBu_4), 1.28 (m, 8H, CH_2 of NBu_4), 0.86 (t, 12H, Me of NBu_4, J_{HH} 7.4), ^{19}F NMR ($CDCl_3$): δ ($CFCl_3$) −120.38 (m, $4F_o$, J_{PtFo} = 459), −165.62 (m, $2F_p$, J_{FpFm} 21.4), −164.77 (m, $4F_m$).

X-ray Crystal Structure Analysis. Suitable crystals of **1** were grown from dichloromethane/hexane. Crystals from **7**·acetone were grown from acetone/hexane. Crystals from **8**·$2H_2O$, **10a**, **11**·CH_2Cl_2·toluene, **12**·0.5(toluene), and **14** were grown from dichloromethane/toluene/hexane. The crystal and molecular structures of the **1**, **7**·acetone, **8**·$2H_2O$, **10a**, **11**·CH_2Cl_2·toluene, **12**·0.5(toluene), and **14** have been determined by X-ray diffraction studies (Tables 4 and 5).

1, **8**·$2H_2O$, and **10a** were measured on a Siemens P4/LT2 machine and **7**·acetone, **11**·CH_2Cl_2·toluene, **12**·1/2toluene, and **14** were measured on a Bruker Smart Apex CCD machine. Graphite monochromated Mo Kα was used. All data were corrected by Lorentz and polarization effects. Absorption corrections were applied for **1**, **8**·$2H_2O$, and **10a** on the basis of Ψ-scans and for **7**·acetone, **11**·CH_2Cl_2·toluene, **12**·0.5(toluene), and **14**, and empirical absorption corrections were also applied.[67]

The structures of **7**·acetone, **11**·CH_2Cl_2·toluene, **12**·0.5(toluene), and **14** were solved by direct methods using *SHELX-97*,[68] which revealed the position of all non-hydrogen atoms, and the structures of **1**, **8**·$2H_2O$, and **10a** were solved by the heavy method. All the structures were refined on F^2 by a full-matrix least-squares procedure using anisotropic displacement parameters for all non-hydrogen atoms. For **1** and **7**·acetone, the hydrogen atom of the amine group of the ligands were located on a difference Fourier map and refined isotropically. The methyl groups were refined using a rigid groups, and the other hydrogens were refined using a riding mode for **1**, **7**·acetone, **8**·$2H_2O$, **10a**, **11**·CH_2Cl_2·toluene, and **12**·0.5(toluene).

(66) Usón, R.; Forniés, J.; Martínez, F. *J. Organomet. Chem.* **1976**, *112*, 105–110.
(67) Sheldrick, G. M. (1996). SADABS. Program for Empirical Absoption Correction of Area Detector Data. University of Götingen, Germany.

Special features:

For **1**: The perchlorate anion is disordered over two sites.

For **8**·$2H_2O$: The structure contains two solvent residues that were tentatively identified as water. Their hydrogens were not included in the refinement.

For **11**·CH_2Cl_2·toluene: One butyl of a NBu_4 is disordered over two positions, ca. 54:46. Its hydrogens were not included in the refinement. The structure contains two solvent residues: the dichloromethane is well-ordered but with a peak of 1.78 eA^3 at 1.79 Å from Cl_1, whereas the other region was tentatively identified as toluene with the highest peak of 3.20 $eÅ^3$ at 2.13 Å from one of its carbon atoms. The additional peaks suggest some solvent disorder. Solvent carbons were refined isotropically. Toluene methyl hydrogens were not included in the refinement.

For **12**: Two methyls of NBu_4 are disordered over two sites. The toluene of solvation is disordered over an inversion center.

For **14**: The hydrogen atoms of the carbons were located in their calculated positions and refined using a riding model. The hydrogen atom of the amine group of one ligand was located on a difference Fourier map and refined isotropically. Molecular graphics were generated using *CAMERON* and *ORTEP-3*.[69]

The unit cell contains two potential solvent-accessible symmetry-related cavities located on the crystallographic inversion centers at (0, 0, $^1/_2$) and ($^1/_2$, $^1/_2$, 0), filled with disordered solvent, probably dichloromethane. The volume of each cavity is 241 $Å^3$. Attempts to model dichloromethane molecules into the solvent density did not result in an acceptable model. As an alternative strategy, the SQUEEZE[70] function of *PLATON*[71] was used to eliminate the contribution of the electron density in the solvent region from the intensity data. The use of this strategy and the subsequent solvent-free model produced slightly better refinement results than the attempt to model the solvent atoms. Therefore, the solvent-free model and intensity data were used for the final results reported here. A total of 88 e was found in each cavity, corresponding to approximately two dichloromethane molecules per cavity. Where relevant, the crystal data reported earlier in this article are given without the contribution of the disordered solvent.

Biological Assays

Circular Dichroism Study. Spectra were recorded at room temperature on an Applied Photophysics Π*-180 spectrometer with a 75 W xenon lamp using a computer for spectral subtraction and smooth reduction. The platinum samples (r_i = 0.1, 0.3, 0.5) were prepared by addition of aliquots of each compound, from stock solutions (1 mg/mL, 2% in DMSO), to a solution of Calf Thymus DNA (Sigma) in TE buffer (20 μg/mL), and incubated for 24 h at 37 °C. As a blank was used a solution of each compound in TE buffer (50 mM NaCl, 10 mM Tris-HCl, 0.1 mM EDTA, pH 7.4). Each sample was scanned twice in a range of wavelengths between 220 and 330 nm. The drawn CD spectra are the means of two independent scans. The ellipticity values are given in millidegrees (mdeg).

Electrophoretic Mobility Study. pB*R*322 plasmid DNA of 0.25 μg/μL of concentration was used for the experiments. Four microlitres of charge maker were added to aliquot parts of 20 μL of the complex/DNA compound containing 0.7 μg of DNA previously incubated at 37 °C for 24 h. The mixtures underwent electrophoresis in a 1% agarose gel in 1x TBE buffer (45 mM Tris-borate, 1 mM EDTA, pH 8.0) for 5 h at 30 V. The gel was subsequently stained in the same buffer containing ethidium bromide (1 μg/mL) for 20 min. The DNA bands were visualized with a Typhoon 9410 Variable Mode Imager (Amersham Biosciences).

Atomic Force Microscopy. Preparation of adducts of DNA−metal complexes. pB*R*322 DNA (25 μg/μL), previously heated at 60 °C, was incubated in an appropriate volume with the required platinum concentration corresponding to the molar ratio r_i = 0.005. The complexes were dissolved in HEPES buffer (40 mM HEPES pH 7.4, and 10 mM $MgCl_2$). The different solutions as well as Milli-Q water were passed through 0.2 nm FP030/3 filters (Schleicher & Schuell GmbH, Germany) and centrifuged at 4000*g* several times to avoid salt deposits and provide a clear background when they were imaged by AFM. The reactions were run at 37 °C for 24 h in the dark.

Sample Preparation for Atomic Force Microscopy. Samples were prepared by placing a drop (3 μL) of DNA solution or DNA-metal complex solution onto green mica (Ashville-Schoonmaker Mica Co., Newport New, VA). After adsorption for 5 min at room temperature, the samples were rinsed for 10 s in a jet of deionized water of 18 MΩ cm^{-1} from a Milli-Q water purification system directed onto the surface with a squeeze bottle. They were then placed into ethanol−water mixture (1:1) five times, plunged three times each in ethanol (100%). The samples were blow dried with compressed argon over silica gel and then imaged in the AFM.

Imaging by Atomic Force Microscopy. The samples were imaged in a Nanoscope III Multimode AFM (Digital Instrumentals Inc., Santa Barbara, CA) operating in tapping mode in air at a scan rate of 1−3 Hz. The AFM probe was a 125 mm long monocrystalline silicon cantilever with integrated conical shaped silicon tips (Nanosensors GmbH Germany) with an average resonance frequency f_o = 330 kHz and spring constant K = 50 N/m. The cantilever is rectangular and the tip radius given by the supplier is 10 nm, with a cone angle of 35° and a high aspect ratio. In general, the images were obtained at room temperature (T = 23 ± 2 °C) and the relative humidity (RH) was typically lower than 40%.

Cell Line and Culture. The T-47D human mammary adenocarcinoma cell line used in this study was grown in RPMI-1640 medium supplemented with 10% (v/v) fetal

(68) Sheldrick, G. M. *SHELX-97, An Integrated System for Solving and Refining Crystal Structures from Diffraction Data*; University of Göttingen: Göttingen, Germany, 1997.
(69) ORTEP-3 Farrugia, L. J. *J. Appl. Crystallogr.* **1997**, *30*, 565.
(70) Sluis, P. van der; Spek, A. L. *Acta Crystallogr.* **1990**, *A46*, 194–201.
(71) Spek, A. L.; *PLATON.* University of Utrecht, The Netherlands, 2001.

bovine serum (FBS) and 0.2 unit/mL bovine insulin in an atmosphere of 5% CO_2 at 37 °C.

Cytotoxicity Assay. Cell proliferation was evaluated by a crystal violet assay. T-47D cells were plated in 96 well sterile plates at a density of 5×10^3 cells/well with 100 μL of medium and were then incubated for 48 h. After attachment to the culture surface, the cells were incubated with various concentrations of the compounds tested freshly dissolved in DMSO and diluted in the culture medium (DMSO final concentration 1%) for 48 h at 37 °C. The cells were fixed by adding 10 μL of 11% glutaraldehyde. The plates were stirred for 15 min at room temperature and then washed 3 to 4 times with distilled water. The cells were stained with 100 μL 1% crystal violet. The plate were stirred for 15 min and then washed 3 to 4 times with distilled water and dried. Acetic acid (100 μL, 10%) were added and the mixture was stirred for 15 min at room temperature. Absorbance was measured at 595 nm in a Tecan Ultra Evolution spectrophotometer.

The effects of complexes were expressed as corrected pertentage inhibition values according to the following equation,

$$\% \text{ inhibition} = [1 - (T/C)] \times 100$$

where T is the mean absorbance of the treated cells and C the mean absorbance in the controls.

The inhibitory potential of compounds was measured by calculating concentration−percentage inhibition curves, these curves were adjusted to the following equation,

$$E = E_{max}/[1 + (IC_{50})/C)^n]$$

where E is the percentage inhibition observed, E_{max} is the maximal effects, IC_{50} is the concentration that inhibits 50% of maximal growth, C is the concentration of compounds tested, and n is the slope of the semilogarithmic dose−response sigmoid curves. This nonlinear fitting was performed using *GraphPad Prism 2.01*, 1996 software (GraphPad Software Inc.).

For comparison purposes, the cytotoxicity of cisplatin was evaluated under the same experimental conditions. All compounds were tested in two independent studies with triplicate points. The in vitro studies were performed at the USEF platform of the University of Santiago de Compostela (Spain).

Conclusions

The first organometallic Pd(II) and Pt(II) complexes with the HmtpO ligand and its anion $mtpO^-$ have been prepared, showing the different coordination modes of this ligand. The structure of $[NBu_4][Pt(C_6F_5)_2(mtpO)(HmtpO)]$ **14** is the first crystal structure of a metal complex containing simultaneously both the neutral HmtpO and the anionic mtpO. In the mtpO−HmtpO metal complexes (**13** and **14**), for the first time, prototropic exchange is observed between the two heterocyclic ligands. The distance metal−N3 observed in the new complexes mainly depends on the nature of the donor atom in the trans position, rather than the neutral or anionic nature of the HmtpO/mtpO ligand. The value of the metal···metal separation in the new dinuclear complexes (**10a**, **11**·CH_2Cl_2·toluene, and **12**·0.5(toluene)) is also a consequence of the trans influence of the ancillary ligands. *cis*-$[Pt(C_6F_5)_2(HmtpO)_2]$·acetone (**7**·acetone) exhibits an H−H orientation of the HmtpO moieties. Strong supramolecular interactions are present in all of the structures. **7**·acetone possesses the shortest distances F_{ortho}···F_{para} observed in fluoroaryl transition metal complexes so far. Circular dichroism, electrophoretic mobility, and atomic force microscopy studies indicate interaction of the new platinum complexes with DNA. Values of IC_{50} were calculated for **2** and **7** against the human tumor cell lines A2780, A2780*cis*R, NCI-H460, and T47D. At 48 h incubation time, both complexes were about 8-fold more active than cisplatin in T47D and show very low resistance factors against an A2780 cell line, which has acquired resistance to cisplatin.

Acknowledgment. This work was supported by the Dirección General de Investigación del Ministerio de Ciencia y Tecnología (Project CTQ2005-09231-C02-01/BQU), Spain, and the Fundación Séneca de la Comunidad Autónoma de la Región de Murcia (Project 00448/PI/04), Spain. We thank Dr. M. J. Prieto for AFM facilities (Universitat de Barcelona), the Screening Unit of the Institute for Industrial Pharmacy of the Universidad de Santiago de Compostela (Spain) for the in vitro studies, and Prof. J. M. Salas (University of Granada, Spain) for helpful discussions.

Supporting Information Available: X-ray crystallography data in CIF format for **1**, **8**·$2H_2O$, **10a**, **7**·acetone, **11**·CH_2Cl_2·toluene, **12**·1/2toluene, and **14**. This material is available free of charge via the Internet at http://pubs.acs.org.

IC701873B